Journal of Visualized Experiments

Primed Mycobacterial Uveitis (PMU) as a model for post-infectious uveitis

--Manuscript Draft--

Article Type:	Methods Article - JoVE Produced Video
Manuscript Number:	JoVE62925R2
Full Title:	Primed Mycobacterial Uveitis (PMU) as a model for post-infectious uveitis
Corresponding Author:	Kathryn Pepple University of Washington UNITED STATES
Corresponding Author's Institution:	University of Washington
Corresponding Author E-Mail:	kpepple@uw.edu
Order of Authors:	Sarah John
	Oliver Bell
	Leslie Wilson
	David Copland
	Kathryn Pepple
Additional Information:	
Question	**Response**
Please specify the section of the submitted manuscript.	Immunology and Infection
Please indicate whether this article will be Standard Access or Open Access.	Open Access ($3900)
Please indicate the **city, state/province, and country** where this article will be **filmed**. Please do not use abbreviations.	Seattle, Washington, USA
Please confirm that you have read and agree to the terms and conditions of the author license agreement that applies below:	I agree to the Author License Agreement
Please provide any comments to the journal here.	
Please confirm that you have read and agree to the terms and conditions of the video release that applies below:	I agree to the Video Release

TITLE:

Primed Mycobacterial Uveitis (PMU) as a Model for Post-Infectious Uveitis

AUTHORS AND AFFILIATIONS:

Sarah John[1], Oliver H. Bell[2], Leslie Wilson[1], David A. Copland[2], Kathryn L. Pepple*[1]

[1]Department of Ophthalmology, University of Washington, Seattle, Washington, United States.
[2]Academic Unit of Ophthalmology, Translational Health Sciences, University of Bristol, Bristol, BS8 1TD, UK.

Email addresses of co-authors:

Sarah John	(sarahj19@uw.edu)
Oliver H. Bell	(Oliver.bell@bristol.ac.uk)
Leslie Wilson	(wunglan8@uw.edu)
David A. Copland	(Dave.copland@bristol.ac.uk)
Kathryn L. Pepple	(kpepple@uw.edu)

*Corresponding author

Kathryn L. Pepple (kpepple@uw.edu)

SUMMARY:

This protocol outlines the steps for inducing Primed Mycobacterial Uveitis (PMU) in mice. This method outlines the steps to help produce reliable and robust ocular inflammation in the mouse model system. Using this protocol, we generated uveitic eyes and uninflamed fellow eyes from single animals for further evaluation with immunologic, transcriptomic, and proteomic assays.

ABSTRACT:

The term 'uveitis' describes a heterogeneous set of conditions that all feature intraocular inflammation. Broadly, uveitis is defined by etiology: infection or autoimmunity. Infectious uveitis requires treatment with the appropriate antimicrobial agents, while autoimmune uveitis requires treatment with corticosteroids or other immunosuppressive agents. Post-infectious uveitis is a form of chronic uveitis that requires corticosteroids to control immune sequela following the initial infection. Uveitis associated with *Mycobacterium tuberculosis* (Mtb) infection is a well-recognized form of post-infectious uveitis, but the mechanisms of disease are not fully understood. To understand the role mycobacterial antigens and innate ligands play in stimulating chronic ocular inflammation following mTB infection, the model Primed Mycobacterial Uveitis (PMU) was developed for use in mice. This manuscript outlines the methods for generating PMU and monitoring the clinical course of inflammation using color fundus and optical coherence tomography (OCT) imaging. PMU is induced by immunization with heat-killed mycobacterial extract followed by intravitreal injection of the same extract into one eye seven days later. Ocular inflammation is monitored longitudinally using in vivo imaging and followed by sample collection for a wide range of assays, including histology, flow cytometry, cytokine analysis, qPCR, or mRNA sequencing. The mouse model of PMU is a useful new tool for studying the ocular responses to

mTB, the mechanism of chronic uveitis, and for preclinical effectiveness tests of new anti-inflammatory therapies.

INTRODUCTION:

The term 'uveitis' describes a heterogeneous set of conditions that all feature intraocular inflammation[1]. Animal models of uveitis are important for understanding disease mechanisms and for preclinical testing of new therapies. A number of animal models of uveitis have been established[2]. The two that have been studied most extensively are experimental autoimmune uveitis (or uveoretinitis; EAU) and endotoxin-induced uveitis (EIU). EAU is typically generated by immunization with ocular antigens or can occur spontaneously when central tolerance is disrupted in the absence of the AIRE gene[3,4]. Other variants of the model have since been developed[5–7] to include different uveitogenic peptides; these have been reviewed extensively[8–10]. EAU is the primary model for forms of T cell-dependent autoimmune uveitis such as Vogt-Koyanagi-Harada disease and birdshot chorioretinitis in humans. EIU is generated by systemic or local injection of bacterial lipopolysaccharide (LPS)[10,11]. EIU has been used as a model of acute uveitis generated by activation of innate immune signaling pathways[12]. Both models have been instrumental to the current understanding of ocular immunology, but neither are effective models for post-infectious chronic uveitis. Recently established in mice, the Primed Mycobacterial Uveitis (PMU) model now provides an approach to interrogate and evaluate clinical and cellular aspects of this form of uveitis[13].

There is a high prevalence of mycobacterial infection worldwide, with over 10 million new cases and more than 1.4 million deaths reported by the World Health Organization in 2019[14]. Extrapulmonary manifestation of active tuberculosis (TB) infection includes uveitis and is a well-recognized cause of infectious uveitis[15,16]. The manifestations of TB-associated uveitis are protean, which likely reflects multiple distinct mechanisms of disease to include direct ocular infection as well as less well-understood immune-mediated inflammation[17–18,19]. The proposed mechanisms for these post-infectious sequelae include a chronic inflammatory response stimulated by the persistence of a pauci-bacillary infection in the retinal pigment epithelium (RPE), a chronic inflammatory response stimulated by the presence of residual pathogen-associated molecular patterns (PAMPs) from a successfully cleared ocular infection, and inappropriate activation of the adaptive immune response against ocular antigens through a process of molecular mimicry or antigen spread caused by systemic TB infection[20–23].

In order to gain a better mechanistic understanding of chronic post-infectious uveitis and study the role of mycobacterial antigens in the initiation of disease, the PMU model was developed for use in mice[13,24]. Accordingly, to elicit inflammation, the mouse first receives a subcutaneous injection of antigen from the heat-killed *Mycobacterium tuberculosis* H37Ra strain to mimic systemic infection, followed seven days later by intravitreal injection of the same antigen administered to the left or right eye to mimic local ocular infection. The intensity and duration of the ensuing uveitis are monitored by longitudinal *in vivo* Optical Coherence Tomography (OCT) and fundal imaging of the eye[25]. PMU is characterized by an acute, myeloid-dominant panuveitis that develops into a chronic T cell-dominant posterior uveitis with vitritis, perivascular retinal inflammation, and focal areas of outer retinal damage[26]. The presence of granulomatous

inflammation in the posterior segment of the eye suggests that the PMU model can be used to study some forms of anterior (granulomatous and non-granulomatous) and intermediate uveitis, seen in patients with immunological evidence of past Mtb infection[27]. Additionally, the components of heat-killed Mtb used in the PMU model have been suggested to trigger immune responses underlying the aspects of recurrent uveitis in patients with ocular tuberculosis who respond to anti-tubercular therapy (ATT)[28]. Due to the differences in disease initiation and inflammatory course when compared to EAU and EIU, PMU represents a new animal model of uveitis that is not dependent on immunization with ocular antigens and may help elucidate mechanisms of disease in patients with chronic uveitis. This protocol outlines the methods for generating PMU, monitoring the clinical course of inflammation, and collecting ocular samples for post-mortem analysis with flow cytometry.

PROTOCOL

All procedures performed were approved locally by the Animal Care and Use Committee at the University of Washington (animal study protocol # 4481-02) or in concordance with the United Kingdom Home Office license (PPL 30/3281) and the University of Bristol Ethical Review Group. Experiments conducted at both institutions were concordant with the Association for Research in Vision and Ophthalmology (ARVO) Statement for the Use of Animals in Ophthalmic and Visual Research. PMU was generated in 6–10-week-old C57BL/6J mice; all mice weighed at least 18 g at the time of uveitis induction and were confirmed negative for the rd8 mutation of the Crb1 gene[29]. Mice were maintained with standard chow and medicated water (acetaminophen 200–300 mg/kg/day) *ad libitum* under specific pathogen-free conditions. Animal euthanasia was performed using a standard carbon dioxide inhalation method[30].

1. Antigen preparation for subcutaneous injection

1.1 Perform all procedures in this section inside a chemical fume hood to prevent inhalation or skin contact with the Mtb H37Ra powder. This includes using chemical-resistant gloves, safety glasses, and protective work clothing (lab coat).

1.2 Use a good sterile technique to prevent contamination of reagents that will be introduced into experimental animals.

1.3 Make the Mtb suspension in PBS by mixing 5 mg of lyophilized, heat-killed *M. tuberculosis* H37Ra powder with 2.5 mL of cold PBS in a 5 mL microcentrifuge tube. Vortex once for 30 s and then place on ice.

1.4 To generate a fine suspension of the H37Ra in PBS, sonicate the suspension on ice for 5 min.

1.4.1. Unclamp the body of the converter unit and clean the probe with a 70% (v/v) alcohol swab.

1.4.2. Switch on the sonicator, adjust the power setting to 4 by turning the power control knob and immerse the probe's tip into the PBS-containing mycobacterial powder. Ensure that the probe tip is immersed to at least half the depth of the sample and that the probe tip is not touching the wall of the microcentrifuge tube.

1.5 Sonicate the mixture on ice for 30 s, pause 30 s and repeat for a total of 5 min to fully disperse the powder into an even suspension without heating the liquid.

1.6 Add 2.5 mL of Freund's Incomplete Adjuvant to the mixture and repeat the sonication process on ice until the emulsion forms a toothpaste-like consistency.

1.7 Set the power to 0 using the control knob and turn off the unit to end the sonication. Remove the tip from the suspension and wipe the probe with an alcohol swab.

1.8 Store the antigen emulsion at 4 °C. Making batches of the emulsion will help ensure consistency across experiments. The emulsion can be stored at 4 °C for up to 3 months.

2. Subcutaneous injection

2.1 Perform subcutaneous injection a week prior to the intravitreal injection (designated as day -7).

2.2 Load a 1 mL syringe (no needle attached) with the mycobacterial emulsion. Due to the viscosity and opacity of the emulsion, difficult-to-see air bubbles can fill the syringe.

2.2.1. To prevent airbubbles in the syringe, after loading 0.2–0.3 mL of emulsion, invert the syringe (tip facing up) and gently tap the syringe repeatedly on the edge of a counter to bring the bubbles to the surface.

2.3 Expel the air from the syringe and continue filling the syringe. Invert and intermittently tap until filled.

2.4 Place a 25 G needle on the syringe and advance the emulsion to fill the needle. Store the syringe on ice until used.

2.5 To perform the subcutaneous injection safely, either anesthetize the mouse or utilize humane restraint methods that allow easy access to the animal hindquarters[31].

2.6 To anesthetize for subcutaneous injection, place the animal in an isoflurane induction chamber (3%–4% for induction and 1%–3% for maintenance). Once anesthetized, ensure that the mouse has a slow respiratory rate and exhibits no signs of respiratory distress.

2.7 Place the subcutaneous injections on either the dorsal surface of the hips, or on the ventral surface of the legs proximal to the region of the inguinal lymph nodes.

2.7.1. Carefully insert the needle to prevent injecting into the muscle. Inject 0.05 mL of the Mtb emulsion into the subcutaneous space. Do not remove the needle immediately in order to allow the thick emulsion to be fully injected.

2.7.2. Repeat the injection on both left and right sides for a total of 0.1 mL per animal.

2.8 If anesthetized, place the mouse on a warm heating pad until complete recovery. Do not leave the mouse unattended until it has regained sufficient consciousness to maintain sternal recumbency.

2.9 Return the mouse to its cage upon complete recovery and label the cage card with the date of subcutaneous injection.

2.10 Provide analgesia with oral acetaminophen (200 mg/kg/day), but not NSAIDs as anti-inflammatory agents can impact the induction of uveitis.

3. Antigen stock preparation for intravitreal injection

3.1 Perform all procedures in this section under appropriate sterile conditions to prevent contamination of the intravitreal Mtb suspension.

3.2 Make the intravitreal suspensions.

3.2.1. For induction of mild to moderate panuveitis, make the intravitreal suspension at a 5 mg/mL concentration by adding 5 mg of the mycobacteria extract to 1 mL of 1x PBS.

3.2.2. For induction of moderate to severe panuveitis, make the intravitreal suspension at a 10 mg/mL concentration by adding 10 mg of the mycobacteria extract to 1 mL of 1x PBS.

3.3 Vortex once for 30 s and then place on ice.

3.4 To generate a fine suspension of the H37Ra in PBS, sonicate the suspension on ice for 10 min as described in step 1.4. Aliquot this stock solution in 100 µL volumes and store at -20 °C.

3.5 Prior to use, thaw at room temperature and vortex on high for 1 min. Keep the aliquots on ice while transport to the animal facility.

4. Intravitreal injection procedure on day 0

4.1. Animal preparation

4.1.1 Wear fitted examination gloves, place the mouse on a weighing balance to obtain its weight in grams.

4.1.2 Give an intraperitoneal injection of 0.02 mL/g bodyweight of a solution containing 100 mg/mL Ketamine and 20 mg/mL Xylazine mixed with sterile water to anesthetize the animal. An alternative approach includes induction using ~1.5% isoflurane (inhaled).

4.1.3 Wait approximately 2 min for the mouse to fall asleep, and then place the mouse in a warming box and cover the lid. Perform pain reflex tests like ear, toe, and tail pinch to assess the depth of anesthesia for the procedure[32].

4.1.4 Once asleep, anesthetize the cornea with 1 drop of 0.5% (v/v) tetracaine. Avoid getting tetracaine near the nose or mouth of the mouse. After 10 s, dab off the excess liquid.

NOTE: It has been observed that iris dilation and anterior chamber (AC) visualization are improved when topical anesthesia is administered, possibly due to improved corneal reflex suppression with the combined systemic and topical anesthesia. However, this step could be omitted if desired.

4.1.5 Dilate the pupil with 1 drop of 2.5% (v/v) phenylephrine. Use caution to avoid any excess droplets that might enter the nose or mouth. After 2–3 min, dab off the excess liquid.

4.1.6 To decrease the risk of endophthalmitis, add 1 drop of 5% betadine to the eye surface and surrounding hair. Leave on the eye for 2–3 min.

NOTE: Perform all procedures in this section under appropriate sterile conditions to prevent endophthalmitis.

4.1.7 Remove betadine and cover the eye with hypromellose (0.3%) or carbomer eye gel 0.2% w/w) to prevent dryness under anesthesia. This will also help prevent cataract formation.

4.2. Setting up the microinjection system

4.2.1 Perform the intravitreal injection using a micropump connected to a microsyringe pump controller and an injection syringe (**Figure 1A–C**). Alternatively, inject with a 33 G needle attached to a Hamilton syringe as described in subsection 4.4.

4.2.2 Connect a 34 G needle to the injection holder to assemble the injector. Loosen the silver screw cap at the front end of the injection holder and slide the needle into the body of the holder about halfway. Tighten the silver screw cap finger tight.

4.2.3 Connect the tubing to the injection holder as mentioned in steps 4.2.4–4.2.5.

4.2.4 To insert the tubing on the injection holder, loosen the plastic screw on the back end of the holder, slide the tubing through the gasket inside and tighten the screw.

4.2.5 Maintain a slight gap with the end of the tubing to prevent tubing damage during the injection. Refer to **Figure 1**C.

4.2.6 Thaw a 100 µL aliquot of the mycobacterium stock suspension.

4.2.7 Add 3 µL of a 1% fluorescein sodium (AK-Fluor) solution and vortex well.

4.2.8 Load a 10 µL syringe with the antigen and fluorescein mix without including any air bubbles.

4.2.9 Remove the loading needle from the syringe, and slide the tubing through the silver screw cap gasket until the tip reaches the zero mark in the syringe body.

4.2.10 Once the tip of the tubing is correctly aligned to the desired position, tighten the screw cap finger tight.

4.2.11 Flush the solution in the syringe through the injection tubing to fully load the system. Then repeat steps 4.2.8–4.2.11 to reload the syringe for injection.

4.2.12 To install the loaded syringe on the micropump, press the clamp release button at the end of the micro-pump to open the syringe clamps.

4.2.13 Position the cap of the plunger into the plunger cap holder at the rear end of the micropump.

4.2.14 Then slide the syringe collar onto the collar stop and the syringe body into the syringe clamp.

4.2.15 Release the clamp button and tighten the plunger retaining screw. Refer to **Figure 1D**.

4.2.16 Slide the injection holder and the needle through the o-clamp on the stereotactic injection apparatus. This is a custom platform; alternatively, the syringe can be held and positioned manually.

4.2.17 Set the infusion volume and the rate of infusion volume on the microsyringe pump controller to inject 500 nL per cycle at a rate of 40 nL/s, respectively.

NOTE: Faster injection rates can be used, however, more reflux may be experienced before needle repositioning can be achieved.

4.2.18 Test the system to ensure correct functioning prior to performing an intravitreal injection.

NOTE: When the injection system is functioning correctly, activation of an injection cycle using the foot pedal or the control pad will produce visible movement of the plunger cap holder and a

308 small droplet of greenish liquid will be seen at the tip of the needle. In the case that no liquid is
309 produced, activate additional cycles or flush and reload the syringe.
310
311 4.2.19 Prior to injecting the eye, gently wipe the needle with a 95% ethanol pad.
312
313 4.3. Intravitreal injection procedure
314
315 4.3.1 The mouse is placed on a stereotaxic apparatus to perform the injection procedure.
316
317 4.3.2 Keep the stage/platform on which the mouse rests warm by attaching 2–3 paper towels
318 on its surface.
319
320 4.3.3 Place the mouse in a prone position on the platform. Use the right and left ear bars to
321 gently fix the animal's head. Refer to **Figure 1E**.
322
323 4.3.4 Position the mouse and orient under the scope so that the superior nasal aspect of the
324 right eye is visible.
325
326 4.3.5 Use a 30 G needle to displace the eyelashes and expose the sclera. Visualize the limbus
327 and the radial blood vessel.
328
329 4.3.6 Use a clean 30 G needle to make a guide hole in the sclera 1–2 mm posterior to the limbus.
330
331 4.3.7 Insert the 34 G needle attached to the injection holder into the eye through the guide
332 hole at an angle that will avoid the lens, but place the needle tip into the vitreous cavity.
333
334 4.3.8 Using the microsyringe pump controller, carefully inject 1 µL of the Mtb extract into the
335 vitreous cavity. In case of consistent reflux, increase the injection volume to 1.5 µL to ensure
336 adequate dose delivery.
337
338 NOTE: For sham controls, inject 1 µL of PBS into the eye of the animal.
339
340 4.3.9 Verify intravitreal placement by visualization of a greenish reflex in the eye. Refer to
341 **Figure 1F**.
342
343 4.3.10 After 10 s, withdraw the needle from the eye. Note any reflux.
344
345 4.3.11 Remove the mouse from the platform, place 0.3% hypromellose or 0.2% w/w carbomer
346 eye ointment on both eyes for corneal protection, and move to the recovery warming box.
347
348 4.3.12 Do not leave the mouse unattended until it has regained sufficient consciousness to
349 maintain sternal recumbency. Do not return to the company of other animals until fully
350 recovered.
351

4.3.13 When the mouse is fully awake, return to the cage and add acetaminophen (200–300 mg/kg/day) medicated water bottle. Label the cage card with the date of IVT injection.

4.4. Alternative method for intravitreal injection

NOTE: This procedure is performed using an operating microscope and a 33 G needle on a microsyringe.

4.4.1 Proptose the eye and hold it in position with a pair of forceps.

4.4.2 Then apply carbomer eye gel 0.2 % w/w or 0.3% hypromellose eye gel and place a circular coverslip (7 mm diameter) over the eye.

4.4.3 Mount a 33 G hypodermic needle on a 5 µL Hamilton syringe and insert it approximately 2 mm circumferential to the corneal limbus with a ~45° injection angle.

4.4.4 Guide the needle bevel into the vitreous, stopping between the lens and the optic disc (from the relative viewpoint of the surgeon, this is above/covering the optic disc – approximately 1.5 mm from the site of insertion), and inject 2 µL of Mtb (at 2.5 ug/µL in PBS) slowly.

4.4.5 Hold the needle in place briefly (to reduce the amount of reflux of injectate) and then remove it.

4.4.6 Post-injection, treat the site with 1% w/w chloramphenicol ointment and reposit the globe by releasing the forceps.

4.4.7 Post-injection, move to the recovery warming box as mentioned in steps 4.3.11–4.3.13.

5. OCT imaging to detect and quantify uveitis

5.1. Animal preparation

5.1.1. Anesthetize the mouse as described in steps 4.1.2–4.1.4

5.1.2. Dilate the pupil with 1 drop 2.5% phenylephrine. Use caution to avoid any excess droplets that might enter the nose or mouth. After 2–3 mins, dab off the excess liquid.

5.1.3. Place 0.3% hypromellose or 0.2% w/w carbomer gel on the eye to prevent dryness while under anesthesia. This will also help to prevent cataract formation.

5.1.4. Wrap the mouse in a layer of surgical gauze to maintain body warmth and place it on the animal cassette. Position the head with the bite bar.

5.2. Acquire the OCT images of the anterior and posterior chambers.

NOTE: If obtaining anterior and posterior chamber images, obtain the posterior chamber (PC) images first to prevent image degradation following cataract formation. Cataract formation can be prevented with frequent lubrication and applying 0.3% hypromellose or 0.2% w/w carbomer eye gel. For extended imaging (>10 min), keeping the mouse warm (through the use of a heat pad) also helps.

5.2.1. After turning on the OCT imaging system, secure the correct imaging lens and adjust the reference arm position as needed.

5.2.2. Open the imaging software, create the unique mouse ID and begin imaging per OCT manufacturer's protocol.

5.2.3. Using the **Free Run** option with the fast scan protocol, position the eye with the optic nerve centered on posterior chamber images or the apex of the cornea on anterior chamber images.

NOTE: **Table 1** contains imaging protocol parameters for two commercially available small animal imaging systems. Refer to **Table of Materials** for product specifications.

5.2.4. For posterior chamber imaging, bring the OCT close to the surface of the eye. Use caution to avoid bringing the surface of the lens in contact with the eye.

5.2.5. Once the eye is correctly positioned, stop the fast scan and select the volume scan protocol, and activate the scan with the **Aim** option.

5.2.6. For posterior segment images, adjust until the optic nerve is centered in the Horizontal B-Scan Alignment image and that the retina is aligned with the Vertical Alignment axis

5.2.7. For anterior segment images, adjust the position to center the apex of the cornea in both the Horizontal B-Scan Alignment image and Vertical Alignment B-Scan Alignment image. The presence of a reflection artifact in both images will confirm proper alignment. Then shift the horizontal image enough to remove the reflection artifact. Refer to **Figure 2**.

5.2.8. Click on **Snapshot** to capture the volume scan image and then click on **Save**.

5.2.9. Next, obtain the averaged central line scan. Open the scan protocol and click on **Aim** followed by **Snapshot**. Right-click on the same panel and then click on **Average**.

5.2.10. Repeat steps 5.2.1–5.2.9 for each eye with both lenses.

5.2.11. After all images are collected, remove the mouse from the cassette and provide corneal protection during recovery as listed in steps 4.3.11–4.3.13.

6. Scoring inflammation by OCT

6.1 Score the OCT images with the help of graders who are masked to the treatment condition.

NOTE: For PMU in the mouse model, the scoring system provided in **Table 2** is recommended.

6.2 If both anterior chamber (AC) and posterior chamber (PC) images were obtained, combine these scores to obtain the final score for each eye.

NOTE: Anterior chamber inflammation resolves before posterior chamber inflammation.

7. Scoring inflammation by post-mortem histology

7.1 At the end of the experiment, collect individual eyes by enucleation, fix in 4% formaldehyde overnight, and proceed for paraffin embedding, sectioning, and H&E staining[33].

NOTE: Multiple 4–8 µm sections along the pupillary-optic nerve axis are recommended.

NOTE: Three sections per eye are scored by a masked grader using the scoring system provided in **Table 3**, and the average score of the three sections is reported as the final histology inflammation score.

REPRESENTATIVE RESULTS:

This protocol demonstrates the induction of uveitis in mice using the primed mycobacterial uveitis model (PMU). Ensuring consistency in the subcutaneous injection and accuracy of the intravitreal injection are key steps in developing the primed mycobacterial uveitis model (PMU). **Figure 1** demonstrates the mouse intravitreal injection procedure using a stereotaxic apparatus. Ear bars help to gently position the head in the same location under the microscope (**Figure 1E**). They also keep the head stable during the intravitreal injection procedure, which decreases the risk of injection trauma. Following a successful injection, fluorescein in the injection solution produces a greenish reflection from within the eye that can be seen under the microscope or from a side view as pictured in **Figure 1F**.

When performed as outlined, the protocol generates robust acute uveitis that can be detected using OCT and fundus imaging as early as 10 h after intravitreal injection. **Figure 2** demonstrates the correct alignment of the eye for OCT imaging. **Table 1A** lists the parameters used in the OCT protocol. A systematic approach to obtaining images will provide high-quality images that can be compared over time. Anterior chamber images are centered on the apex of the cornea using the en face SLO image (**Figure 2A**) with the iris aligned in parallel to both the horizontal and vertical planes (**Figure 2B,C**). Volume and line scans are captured with a vertical alignment such that inferior and superior regions can be viewed simultaneously. Posterior segment images are centered on the optic nerve using the en face SLO image (**Figure 2D**), and the bright band of the RPE is used to align the retina in parallel to both the horizontal and vertical planes (**Figure 2E,F**).

Figure 3 shows typical findings of PMU ocular inflammation using OCT imaging. Twenty four hours after intravitreal injection, inflammatory cells are seen in the aqueous and vitreous (**Figure 3B**). In the presence of moderate or severe inflammation, a hypopyon will be seen in the inferior angle in the AC. The degree of ocular inflammation can be scored on these OCT images using the criteria listed in **Table 2**. Representative examples of images demonstrating the inflammatory features typical for each score are shown in **Figure 4**. AC and PC chamber scores can be added together to generate the combined OCT score. Combined scores >0 but ≤2.5 represent mild inflammation. Moderate inflammation is determined by scores >2.5 but ≤4.5. Scores >4.5 identify severe inflammation. Inflammation typically peaks 48 h after intravitreal injection with OCT scores in the AC and PC between 1 and 3 (Combined scores between 2 and 6). AC and PC scores of 0.5 or 4 are less common. In the case scores outside the typical range are encountered frequently, troubleshooting may be required to identify the factors contributing to outlier scores (see discussion section). Inflammation scores in the anterior chamber tend to return to zero within one week following intravitreal injection. In contrast, posterior scores do not return to zero; instead, low-level chronic inflammation persists in the form of vitritis, and perivascular lymphocytes infiltrate in the retina for 1–2 months following intravitreal injection.

Inflammation score in PMU can also be determined using histology. **Figure 5** shows representative H&E sections for use in scoring the severity of PMU by histology. The number of inflammatory cells in the aqueous and vitreous are counted and used to determine the severity using the score criteria listed in **Table 3**. Inflammatory cell infiltration of the ciliary body is commonly seen on one side of the histology section (unilateral involvement) in mild or moderate inflammation. When inflammation is severe, this is reflected by the presence of an inflammatory cell infiltrate in the ciliary body on both sides of the lens (termed bilateral involvement). During later time points after intravitreal injection, chronic inflammation manifestations, including the presence of perivascular and intraretinal leukocytes and outer retinal folds, can also be identified. Histology can also be helpful in identifying eyes impacted by poor injection techniques. Trauma to the lens during the intravitreal injection can be identified by the presence of amorphous eosin-stained (pink) lens proteins outside the lens capsule adjacent to the area of trauma. Reflux of the intravitreal mTB into the subconjunctival space will generate inflammation outside the eye that can be identified by a careful review of periocular structures present on the sections. Due to the failure to retain mTB extract within the eyes, these eyes will typically have low OCT scores of inflammation.

Brightfield fundus imaging can also be used to identify clinically relevant aspects of PMU, including the development of a hypopyon, vitritis, and retinal or perivascular inflammatory cell infiltration. **Figure 6** shows two examples where retinal and perivascular inflammation can be seen on fundus images. These two eyes also show the range of inflammation that is common in the PMU model. **Table 1B** lists the parameters used in the fundus/ retinal OCT imaging system. Note the impact that severe inflammation has on the image quality (**Figure 6**, day 2, OCT and fundus images in the top row) and the extent of disease present on day 21. Corneal edema can also decrease image quality during acute inflammation; however, it is uncommon for corneal edema to be severe from inflammation alone. More commonly, the image quality will be

528 degraded by epithelial damage resulting from incomplete surface protection during imaging and
529 anesthesia events.
530
531 The PMU model can be used to induce uveitis in any mouse breed or genotype. In albino eyes,
532 OCT can still be used to score inflammation, but the absence of fundus pigment makes
533 visualization of inflammation challenging by brightfield imaging[13,34]. Post mortem studies can be
534 performed on ocular tissues, regional lymph nodes, or the spleen. Some examples include assays
535 for the presence of immune cells such as flow cytometry and immunohistochemistry and
536 measurement of inflammatory cytokines. At all time points tested after initiation of inflammation
537 with PMU (day 1 to day 56), there are sufficient $CD45^+$ inflammatory cells present in individual
538 eyes to detect many major leukocyte populations in the eye by multi-parameter flow analysis[12,35].
539 Aqueous (2–5 µL) and vitreous (5–10 µL) can be collected from inflamed eyes for protein
540 concentration determination, proteomic studies, or cytokine concentration determination[36].
541
542 **FIGURE AND TABLE LEGENDS**
543 **Figure 1: Mouse intravitreal injection set up.** The intravitreal injection is performed on the
544 mouse eye using (**A**) a microsyringe pump controller connected to the (**B**) Micropump and (**C**) an
545 injection syringe. The syringe is loaded and mounted on the (**D**) Micropump. The mouse head is
546 positioned using (**E**) ear bars to ensure stability and consistency during the intravitreal injection
547 procedure. (**F**) Fluorescein in the injection solution produces a greenish reflection from within
548 the eye after a successful procedure.
549
550 **Figure 2: Proper alignment of the eye for OCT imaging.** (**A**) Using the en-face scanning laser
551 ophthalmoscope (SLO) image, the eye is centered for anterior chamber imaging. The green line
552 indicates the position of the horizontal line scan shown in panel (**B**). Note that the central cornea
553 is avoided to decrease reflection artifact. (**C**) Vertical B-Scan through the paracentral anterior
554 chamber. This scan is obtained at 90° from the horizontal scan. Note that the alignment of the
555 iris sections on each side of the lens is level in the horizontal scan (panel B) and arranged one
556 above the other in the vertical scan (panel C). (**D**) Using the SLO image, the posterior chamber
557 image is centered on the optic nerve. (**E**) Horizontal B-Scan Alignment, (**F**) Vertical B-Scan
558 Alignment.
559
560 **Figure 3: Induction of PMU generates panuveitis that can be monitored by longitudinal OCT**
561 **imaging.** The top row shows anterior chamber (AC); the bottom row shows posterior chamber
562 (PC) OCT images to highlight pathological changes in the disease course. (**A**) Baseline OCT image
563 of the AC (top) and PC (bottom) prior to induction of uveitis, both score 0. (**B**) Day 1 after
564 intravitreal injection showing the presence of corneal edema (black arrow), a hypopyon (*)
565 multiple free-floating inflammatory cells in the AC (white arrows), and vitritis (white arrowheads)
566 in the PC. (**C**) Day 7 after intravitreal injection with few AC cells on the anterior lens capsule (white
567 arrow) and decreased vitritis (white arrowhead). (**D**) Day 28 after intravitreal injection anterior
568 chamber with resolved AC inflammation and mild vitritis. Abbreviations: C- cornea, L – lens, I –
569 iris, Aq - aqueous, V vitreous, RGC – retinal ganglion cells, PR – photoreceptors, Ch- choroid.
570

571 **Figure 4: OCT score examples.** An OCT score between 0 and 4 is assigned to each AC image and
572 PC image using the categorical system shown in **Table 2**. The AC and PC scores are combined for
573 the final OCT score for the eye. (**A**,**D**) Examples of a score of zero. (**B**,**E**) Examples of a score of
574 0.5. (**C,F**) Examples of a score of 1. (**G**,**J**) Examples of a score of 2. (**H**,**K**) Examples of a score of 3.
575 (**I**,**L**) Examples of a score of 4 are shown in panels **I** and **L**.
576
577 **Figure 5: Histology score examples.** Histology score is determined based on five characteristics
578 visible in H&E sections: Anterior chamber protein density, anterior chamber cell number,
579 immune cell infiltration of the ciliary body, vitreous cell density, retinal vascular inflammation,
580 and structural retinal changes. A score of 0–2 is assigned for each characteristic. The description
581 of each score is found in **Table 3**. A representative example score of 0–2 for each characteristic
582 is shown in this figure. The left column demonstrates the score of zero. The center column shows
583 examples of score 1. The right column shows examples of score 2. A score of 2 for ciliary body
584 score is assigned if the ciliary body on either side of the lens in the same section demonstrates
585 cellular inflammation. The final histology score is the sum of the score for each of the five criteria
586 (max score 10). The arrow in the bottom right panel indicates perivascular leukocytes associated
587 with a superficial retinal vessel. Black scale bar indicates 500 µm. Ciliary scale bars indicate 100
588 µm.
589
590 **Figure 6: Longitudinal fundus imaging in PMU identified a range of disease severity.** (**A**)
591 Severely inflamed eyes demonstrate multiple white infiltrates in the retina and vascular
592 tortuosity on color fundus imaging (top row) as well as dense vitritis and retinal edema on OCT
593 (bottom row) on day 2. Progression in the number of retinal lesions can be seen over time while
594 the vitritis improves. Green line indicates the position of the OCT image. (**B**) Mildly inflamed eyes
595 demonstrate fewer and more discrete linear lesions in the fundus and a number of infiltrating
596 cells in the vitreous space. Scale bar = 100 µm.
597
598 **Table 1: Scan parameters.** (**A**) OCT scan parameters. (**B**) Fundus/retinal OCT scan parameters
599
600 **Table 2: PMU OCT score criteria:** OCT images are scored according to the criteria listed in the
601 table. AC and PC scores are added to obtain the final score of the eye. In cases where a clear view
602 of the eye was not acquired, a score of NA was assigned to the images, and these were excluded
603 from the study.
604
605 **Table 3: PMU histology score criteria:** H&E sections of the eye were scored based on the criteria
606 listed in the table. Three sections from the same eye were scored and averaged to obtain the
607 final histology score of the eye.
608
609 **DISCUSSION:**
610 Animal models of uveitis have been instrumental in understanding the mechanisms of ocular
611 inflammation and homeostasis as well as enabling preclinical evaluation of medical and surgical
612 therapies for patients with uveitis[37]. Both rabbit and rat variants of the PMU model have
613 demonstrated their value in preclinical therapy via proof of concept studies[38–40]. Due to the
614 availability of a diverse range of transgenic strains in mice, establishing the mouse PMU model

system now permits more detailed mechanistic studies to identify specific cell types, pathways, and genes that contribute to the pathology of this disease.

Animal models of uveitis can demonstrate animal to animal variability in the incidence and intensity of inflammation[41]. In the C57BL/6 mouse strain, PMU is reliably generated using the protocol outlined here. Strain-specific variations in uveitis course and intensity have been reported for both EAU and EIU[42,43]. While strain-specific impacts on severity and course of PMU have not been measured experimentally, this model has been used in wild-type C57BL/6J as well as in albino mice (B6(Cg)-Tyrc-2J/J) and produced similar inflammatory responses. In generating the PMU model, controlling the considerations listed below can help new researchers limit variability and produce the most consistent and reproducible uveitis.

Ensure consistency in the subcutaneous injections:
To provide a consistent subcutaneous injection, ensure that all air bubbles are removed from the emulsion. Considerations include a short centrifuge (30 s at 400 x *g*) of the premade emulsion prior to loading the syringe. This will remove air trapped in the emulsion. Also, when loading the syringe, periodically invert (tip-up) and tap the syringe to remove any air bubbles. While injecting, do not place the syringe too deep in order to avoid intramuscular injection. Conversely, a shallow (intradermal) injection can result in erosion of the emulsion through the skin. Remember to pause briefly before removing the syringe from the injection site to ensure complete injection of the thick viscous emulsion and to prevent reflux from the skin.

Seven days after placing the subcutaneous injection, confirm the presence of palpable nodules on either side of the hind legs. If no nodules can be identified, it is possible that air was injected rather than emulsion. In this case, acute inflammation may not be as robust, and chronic inflammation may not develop.

Prevent the development of infectious endophthalmitis:
Bacterial or fungal endophthalmitis will generate a confounding variable if not prevented[44]. In order to prevent bacterial endophthalmitis, always practice good aseptic technique when making the intravitreal suspension, handling, and cleaning all reusable tools that will come in contact with the eye. Using sterile single-use items, autoclaving, or cleaning with 95% alcohol washes or wipes is important. Appropriate use of betadine applied to the ocular surface, lids, and periocular fur will also help prevent endophthalmitis[45]. It is straightforward to recognize an eye with infection as the ocular structures will be obliterated by extreme inflammation during the post-injection course. This is not typical for PMU. The presence of intraocular bleeding can also suggest endophthalmitis or trauma from the injection. In such cases, exclude these animals from the study.

Ensure consistency in the intravitreal injection:
The intravitreal injection is a critical step in the induction of reliable and reproducible inflammation in PMU. Providing a consistent amount of Mtb suspension with each injection, avoiding trauma, and preventing reflux of the suspension are all factors that should be considered when performing the injections. To ensure a consistent suspension, vortex the stock

659 suspension thoroughly upon thawing and before loading it in the syringe. Since this Mtb extract
660 used does not form a solution, the suspension can undergo sedimentation over time. To ensure
661 uniform concentration of the Mtb extract in each injection, use or expel and reload the syringe
662 within 15 minutes of loading. Phenylephrine is used for dilation to provide a larger field of view
663 to the posterior eye and reduce the risk of trauma to the eye during the injection. This drop
664 generates natural lid retraction and slight proptosis of the globe, allowing good visualization of
665 area 1–2 mm posterior to the limbus without the need to grasp the eye with forceps. Using
666 forceps to restrain the eye could cause potential trauma and transiently increase intraocular
667 pressure and the risk of reflux of the Mtb suspension. Trauma can also be caused by attempting
668 to inject too much volume into the eye. The injection volume is limited to 2 µL to prevent
669 significant and prolonged elevation of intraocular pressure and trauma to the eye. Additionally,
670 younger animals will have eyes that are smaller than adult mice. Typically 6–8 week mice (20–25
671 g) provide a uniform eye size and ensure greater consistency in the inflammation following
672 injection of Mtb. A higher frequency of post-injection reflux of the mycobacterial suspension was
673 observed in smaller mice. This, in turn, leads to a less-than-expected acute inflammation. A dilute
674 fluorescein solution is used to provide the novice injector visual feedback on the success of their
675 injection technique. Dilation at the time of injection will allow for direct visualization of the
676 injected material in the vitreous cavity and the opportunity to note any evidence of lens trauma.
677 In the case of lens trauma, it can cause a change in lens clarity that will cause a cataract which
678 can be visualized on OCT. In the case of ocular trauma, the eyes need to be excluded from the
679 study due to the possibility of lens-induced uveitis[46]. We recommend pausing for 10 s before
680 removing the syringe from the eye to allow dispersion of the Mtb suspension within the eye and
681 decrease reflux.
682
683 The PMU model can be modified to change the intensity of acute inflammation by varying the
684 concentration of the Mtb in the intravitreal injection. Different dosages ranging from 2.5 µg/µL
685 to 15 µg/µL have been tested previously in our lab. However, doses higher than 10 µg/µL were
686 found to cause severe eye damage, including spontaneous lens rupture, severe corneal edema
687 and scarring, and hyphema. This degree of severity is not typical in human patients with post-
688 infectious uveitis, and therefore, these concentrations are not recommended. A 5 µg/µL dose
689 was found to reliably produce mild to moderate acute inflammation and mild chronic uveitis; the
690 10 µg/µL dose produces a reliably moderate to severe acute disease and more notable chronic
691 disease. Thus, varying the intravitreal concentration can provide alternative disease severities for
692 use as needed based on the experimental question. Controls should be selected to ensure results
693 are due to the response to mTB and not trauma associated with the subcutaneous or intravitreal
694 injections. In the sham injection controls, PBS can be used in place of the mTB extract. For
695 comparisons to unexposed animals, true naive samples should be considered as fellow eyes are
696 not always equivalent.
697
698 Due to the small size of the mouse eye, OCT can be a more sensitive assay to detect inflammation
699 in the anterior chamber than direct visualization or microscopic bright field photography. Prior
700 work with PMU in rats[25] determined that more cells can be detected by histology than by OCT
701 but that there is a good correlation between the two modalities. OCT has the added advantage
702 that it can be used to monitor the inflammation longitudinally in the same animal. Other major

703 mouse models of uveitis, such as EAU and EIU, have also employed OCT for quantitative
704 analysis[12,47,48]. In the PMU model of mice, anterior chamber cells are only visible on OCT and
705 cannot be seen on clinical exams unless a large hypopyon is present. Vitreous inflammation
706 (vitritis) can be observed with color fundus imaging, but detecting quantitative change is possible
707 only with OCT imaging. Other aspects of the model, such as retinal vascular inflammation and
708 retinal damage, can be easily identified with either OCT and microscopic brightfield fundus
709 photography.
710
711 When using OCT, it is important to consider how localized imaging can be impacted by regional
712 differences in the degree of inflammation. Prior reports have identified an uneven distribution of
713 cells in the anterior chamber of humans, with more cells located inferiorly[49]. In mice, a similar
714 predisposition is common. Thus, vertical or radial scans through the AC will help ensure images
715 that capture the range of inflammation. Additionally, performing imaging in the same place will
716 also provide consistency to images collected in the same eye longitudinally. To obtain images in
717 the same part of the eye, use stable landmarks and a systematic approach. For anterior chamber
718 images, the image is centered immediately adjacent to the apex of the cornea and oriented
719 vertically so that the presence of a hypopyon can be detected in the inferior angle. For posterior
720 segment images, the image is centered on the optic nerve. It is recommended to consider using
721 at least 3 line scans for scoring to ensure regional variability is captured. In cases where
722 inflammation is restricted to peripheral locations, acquiring volume scans can be helpful. The
723 collection of volume scans can also help capture regional variations but will increase data storage
724 requirements.
725
726 Other *in vivo* assays that can be used to characterize inflammation in the PMU mouse model
727 include bioluminescence imaging[13,35]. Post-mortem assays like multi-parameter flow cytometric
728 analysis can be performed to identify and quantify infiltrating immune cell type populations in
729 the aqueous and posterior chamber of the eye[12,26]. In the PMU model, acute inflammation is
730 characterized by an innate response with a predominant neutrophil infiltrate, followed by a
731 chronic and persistent adaptive T cell dominant response that persists for over a month[35]. Other
732 assays of immune function that can be performed on post-mortem tissues include ocular fluid
733 cytokine analysis. Additionally, other downstream assays like mRNA sequencing and
734 immunofluorescence imaging can be used to assess gene and protein expression patterns of
735 retinal immune cell populations in uveitis[50,51].
736
737 The PMU model can be replicated in other rodent systems using adaptations appropriate for the
738 different species. PMU model has been previously used in rats and rabbits[38–40]. In rats, acute
739 panuveitis develops following intravitreal injection that resolves spontaneously over 14 days
740 without developing signs of chronic inflammation by histology[24]. In rabbits, induction of uveitis
741 utilizes two rounds of subcutaneous injection prior to intravitreal injection but also generates a
742 robust panuveitis. One of the advantages of using the mouse model is the ready availability of
743 numerous transgenic and knockout strains that can help understand the basic mechanism of
744 uveitis[52]. All rodent models can be used for preclinical therapy testing if the agent is administered
745 systemically or as a topical drop. However, due to their larger size, rat and rabbit eyes are better

models for use in preclinical studies of implantable or local injection treatment options for uveitis.

In summary, this protocol provides researchers interested in studying the mechanisms of chronic ocular inflammation with a new tool that is not dependent on prior immunization with ocular antigens.

ACKNOWLEDGMENTS

This work is supported by funding from the National Institutes of Health, Bethesda, Maryland, United States (KP) K08EY0123998, (KP) R01EY030431, (KP) R21 EY02939, UW vision research core grant (NEI P30EY01730), gifts from the Mark Daily, MD Research Fund and the Christopher and Alida Latham Research fund, an unrestricted departmental grant from Research to Prevent Blindness, and career development award from Research to Prevent Blindness (KP). The work conducted in Bristol was supported by additional funding from Sight Research UK and The Underwood Trust.

DISCLOSURES

The authors have no financial conflicts to disclose.

REFERENCES

1. Aao *2019-2020 Basic and Clinical Science Course, Section 09: Uveitis and Ocular Inflammation*. American Academy of Ophthalmology. (2019).
2. Caspi, R. R. Animal models of autoimmune and immune-mediated uveitis. *Drug Discovery today. Disease Models*. **3** (1), 3–9 (2006).
3. DeVoss, J. et al. Spontaneous autoimmunity prevented by thymic expression of a single self-antigen. *The Journal of Experimental Medicine*. **203** (12), 2727–2735 (2006).
4. Caspi, R. R. et al. A new model of autoimmune disease. Experimental autoimmune uveoretinitis induced in mice with two different retinal antigens. *Journal of Immunology* . **140** (5), 1490–1495 (1988).
5. Tang, J., Zhu, W., Silver, P. B., Su, S. -B., Chan, C. -C., Caspi, R. R. Autoimmune uveitis elicited with antigen-pulsed dendritic cells has a distinct clinical signature and is driven by unique effector mechanisms: Initial encounter with autoantigen defines disease phenotype. *The Journal of Immunology*. **178** (9), 5578–5587 (2007).
6. Broekhuyse, R. M., Kuhlmann, E. D., Winkens, H. J. Experimental melanin-protein induced uveitis (EMIU) is the sole type of uveitis evoked by a diversity of ocular melanin preparations and melanin-derived soluble polypeptides. *Japanese Journal of Ophthalmology*. **40** (4), 459–468 (1996).
7. Pennesi, G. et al. A humanized model of experimental autoimmune uveitis in HLA class II transgenic mice. *The Journal of Clinical Investigation*. **111** (8), 1171–1180 (2003).
8. Caspi, R. R. Understanding autoimmune uveitis through animal models. The Friedenwald lecture. *Investigative Ophthalmology & Visual Science*. **52** (3), 1872–1879 (2011).
9. Bansal, S., Barathi, V. A., Iwata, D., Agrawal, R. Experimental autoimmune uveitis and other animal models of uveitis: An update. *Indian Journal of Ophthalmology*. **63** (3), 211–218 (2015).

790 10. Smith, J. R., Hart, P. H., Williams, K. A. Basic pathogenic mechanisms operating in
791 experimental models of acute anterior uveitis. *Immunology and Cell Biology*. **76** (6), 497–512
792 (1998).
793 11. Rosenbaum, J. T., McDevitt, H. O., Guss, R. B., Egbert, P. R. Endotoxin-induced uveitis in
794 rats as a model for human disease. *Nature*. **286** (5773), 611–613 (1980).
795 12. Chu, C. J. et al. Multimodal analysis of ocular inflammation using the endotoxin-induced
796 uveitis mouse model. *Disease Models & Mechanisms*. **9** (4), 473–481 (2016).
797 13. Gutowski, M. B., Wilson, L., Van Gelder, R. N., Pepple, K. L. In vivo bioluminescence
798 imaging for longitudinal monitoring of inflammation in animal models of uveitis. *Investigative*
799 *Ophthalmology & Visual Science*. **58** (3), 1521–1528 (2017).
800 14. *Global tuberculosis report 2019*. World Health Organization, (2019).
801 15. Biswas, J., Badrinath, S. S. Ocular morbidity in patients with active systemic tuberculosis.
802 *International Ophthalmology*. **19** (5), 293–298 (1995).
803 16. Donahue, H. C. Ophthalmologic experience in a tuberculosis sanatorium. *American*
804 *Journal of Ophthalmology*. **64** (4), 742–748 (1967).
805 17. El-Asrar, M. A., Abouammoh, M., Al-Mezaine, H. S. Tuberculous uveitis. *Middle East*
806 *African Journal of Ophthalmology*. **16** (4), 188–201 (2009).
807 18. Bodaghi, B. et al. Chronic severe uveitis: etiology and visual outcome in 927 patients from
808 a single center. *Medicine*. **80** (4), 263–270 (2001).
809 19. Cunningham, E. T., Jr, Forrester, J. V., Rao, N. A., Zierhut, M. Post-infectious uveitis. *Ocular*
810 *Immunology and Inflammation*. **24** (6), 603–606 (2016).
811 20. Wroblewski, K. J., Hidayat, A. A., Neafie, R. C., Rao, N. A., Zapor, M. Ocular tuberculosis: a
812 clinicopathologic and molecular study. *Ophthalmology*. **118** (4), 772–777 (2011).
813 21. Yeh, S., Sen, H. N., Colyer, M., Zapor, M., Wroblewski, K. Update on ocular tuberculosis.
814 *Current Opinion in Ophthalmology*. **23** (6), 551–556 (2012).
815 22. Tagirasa, R., Parmar, S., Barik, M. R., Devadas, S., Basu, S. Autoreactive T cells in
816 immunopathogenesis of TB-associated uveitis. *Investigative Ophthalmology & Visual Science*. **58**
817 (13), 5682–5691 (2017).
818 23. Agrawal, R. et al. Insights into the molecular pathogenesis of ocular tuberculosis.
819 *Tuberculosis* . **126**, 102018 (2021).
820 24. Pepple, K. L. et al. Primed mycobacterial uveitis (PMU): Histologic and cytokine
821 characterization of a model of uveitis in rats. *Investigative Ophthalmology & Visual Science*. **56**
822 (13), 8438–8448 (2015).
823 25. Pepple, K. L., Choi, W. J., Wilson, L., Van Gelder, R. N., Wang, R. K. Quantitative assessment
824 of anterior segment inflammation in a rat model of uveitis using spectral-domain optical
825 coherence tomography. *Investigative Ophthalmology & Visual Science*. **57** (8), 3567–3575 (2016).
826 26. Pepple, K. L., Wilson, L., Van Gelder, R. N. Comparison of aqueous and vitreous
827 Lymphocyte populations from two rat models of experimental uveitis. *Investigative*
828 *Ophthalmology & Visual Science*. **59** (6), 2504–2511 (2018).
829 27. Basu, S., Elkington, P., Rao, N. A. Pathogenesis of ocular tuberculosis: New observations
830 and future directions. *Tuberculosis* . **124**, 101961 (2020).
831 28. Basu, S., Rao, N., Elkington, P. Animal models of ocular tuberculosis: Implications for
832 diagnosis and treatment. *Ocular Immunology and Inflammation*. 1–7 (2020).
833 29. Mattapallil, M. J. et al. The Rd8 mutation of the Crb1 gene is present in vendor lines of

834 C57BL/6N mice and embryonic stem cells, and confounds ocular induced mutant phenotypes.
835 *Investigative Ophthalmology & Visual Science*. **53** (6), 2921–2927 (2012).
836 30. Underwood, W., Anthony, R. AVMA guidelines for the euthanasia of animals: 2020
837 edition. **2013** (30), 2020–2021 (2020).
838 31. Donovan, J., Brown, P. Handling and restraint. *Current protocols in immunology.* edited
839 by John E. Coligan [et al.]. **Chapter 1**, Unit 1.3, John Wiley & Sons, Inc. (2006).
840 32. Tremoleda, J. L., Kerton, A., Gsell, W. Anaesthesia and physiological monitoring during in
841 vivo imaging of laboratory rodents: considerations on experimental outcomes and animal
842 welfare. *EJNMMI Research*. **2** (1), 44 (2012).
843 33. Cardiff, R. D., Miller, C. H., Munn, R. J. Manual hematoxylin and eosin staining of mouse
844 tissue sections. *Cold Spring Harbor protocols*. **2014** (6), 655–658 (2014).
845 34. Paques, M. et al. Panretinal, high-resolution color photography of the mouse fundus.
846 *Investigative Ophthalmology & Visual Science*. **48** (6), 2769–2774 (2007).
847 35. John, S., Rolnick, K., Wilson, L., Wong, S., Van Gelder, R. N., Pepple, K. L. Bioluminescence
848 for in vivo detection of cell-type-specific inflammation in a mouse model of uveitis. *Scientific*
849 *Reports*. **10** (1), 11377 (2020).
850 36. Fortmann, S.D., Lorenc, V.E., Hackett, S., Campochiaro, P.A. Murine Vitreous Tap
851 (MurViTap): a novel technique to extract uncontaminated mouse vitreous humor, quantify
852 retinal vascular permeability, and compare proteins secreted by diseased and normal retina.
853 *Investigative ophthalmology & visual science*. **58** (8), 5978–5978 (2017).
854 37. Caspi, R. R. Understanding autoimmunity in the eye: from animal models to novel
855 therapies. *Discovery Medicine*. **17** (93), 155–162 (2014).
856 38. Mruthyunjaya, P. et al. Efficacy of low-release-rate fluocinolone acetonide intravitreal
857 implants to treat experimental uveitis. *Archives of Ophthalmology*. **124** (7), 1012–1018 (2006).
858 39. Jaffe, G. J., Yang, C. S., Wang, X. C., Cousins, S. W., Gallemore, R. P., Ashton, P. Intravitreal
859 sustained-release cyclosporine in the treatment of experimental uveitis. *Ophthalmology*. **105** (1),
860 46–56 (1998).
861 40. Pepple, K. L. et al. Uveitis therapy with shark variable novel antigen receptor domains
862 targeting tumor necrosis factor alpha or inducible t-cell costimulatory ligand. *Translational Vision*
863 *Science & Technology*. **8** (5), 11 (2019).
864 41. Mattapallil, M. J. et al. Characterization of a New epitope of IRBP that induces moderate
865 to severe uveoretinitis in mice with H-2b haplotype. *Investigative Ophthalmology & Visual*
866 *Science*. **56** (9), 5439–5449 (2015).
867 42. Silver, P. B., Chan, C. C., Wiggert, B., Caspi, R. R. The requirement for pertussis to induce
868 EAU is strain-dependent: B10.RIII, but not B10.A mice, develop EAU and Th1 responses to IRBP
869 without pertussis treatment. *Investigative Ophthalmology & Visual Science*. **40** (12), 2898–2905
870 (1999).
871 43. Li, Q., Peng, B., Whitcup, S. M., Jang, S. U., Chan, C. C. Endotoxin induced uveitis in the
872 mouse: susceptibility and genetic control. *Experimental Eye Research*. **61** (5), 629–632 (1995).
873 44. Astley, R. A., Coburn, P. S., Parkunan, S. M., Callegan, M. C. Modeling intraocular bacterial
874 infections. *Progress in Retinal and Eye Research*. **54**, 30–48 (2016).
875 45. Lau, P. E., Jenkins, K. S., Layton, C. J. Current evidence for the prevention of
876 endophthalmitis in anti-VEGF intravitreal injections. *Journal of Ophthalmology*. **2018**, 8567912
877 (2018).

878 46. Nche, E. N., Amer, R. Lens-induced uveitis: an update. *Graefe's Archive for Clinical and*
879 *Experimental Ophthalmology*. **258** (7), 1359–1365 (2020).
880 47. Chu, C. J. et al. Assessment and in vivo scoring of murine experimental autoimmune
881 uveoretinitis using optical coherence tomography. *PLoS ONE*. **8** (5), e63002 (2013).
882 48. Harimoto, K., Ito, M., Karasawa, Y., Sakurai, Y., Takeuchi, M. Evaluation of mouse
883 experimental autoimmune uveoretinitis by spectral domain optical coherence tomography. *The*
884 *British Journal of Ophthalmology*. **98** (6), 808–812 (2014).
885 49. Li, Y., Lowder, C., Zhang, X., Huang, D. Anterior chamber cell grading by optical coherence
886 tomography. *Investigative Ophthalmology & Visual Science*. **54** (1), 258–265 (2013).
887 50. Bell, O. H. et al. Single eye mRNA-seq reveals normalisation of the retinal microglial
888 transcriptome following acute inflammation. *Frontiers in Immunology*. **10**, 3033 (2019).
889 51. Lipski, D. A. et al. Retinal endothelial cell phenotypic modifications during experimental
890 autoimmune uveitis: a transcriptomic approach. *BMC Ophthalmology*. **20** (1), 106 (2020).
891 52. Agarwal, R. K., Silver, P. B., Caspi, R. R. *Rodent Models of Experimental Autoimmune*
892 *Uveitis*. In: Perl A. (eds) *Autoimmunity. Methods in Molecular Biology (Methods and Protocols),*
893 900, 443–469. Humana Press, Totowa, NJ (2012).
894
895

Figure 1

Click here to access/download;Figure;Figure 1.jpg

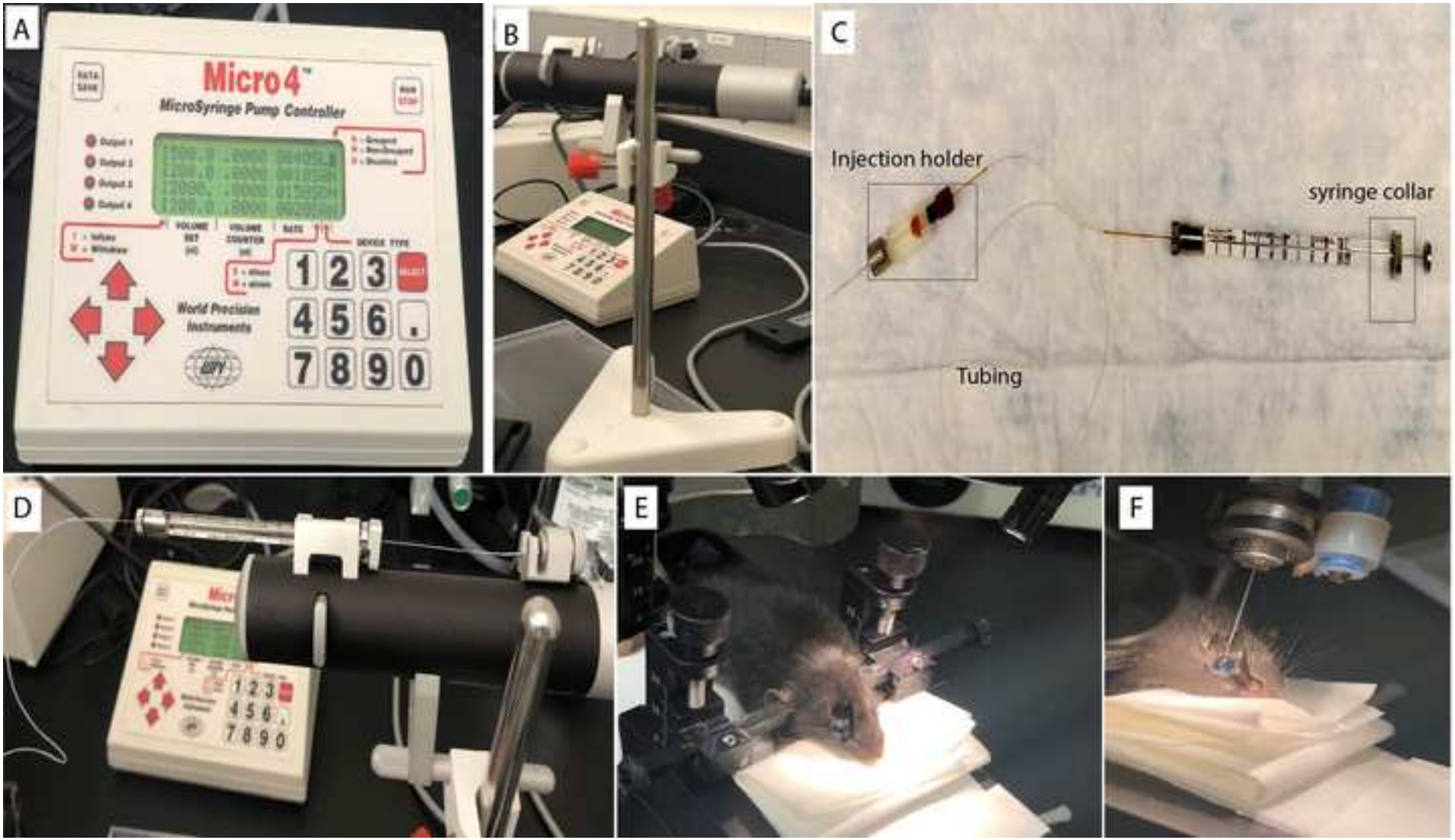

Figure 2

Click here to access/download;Figure;Figure 2.jpg

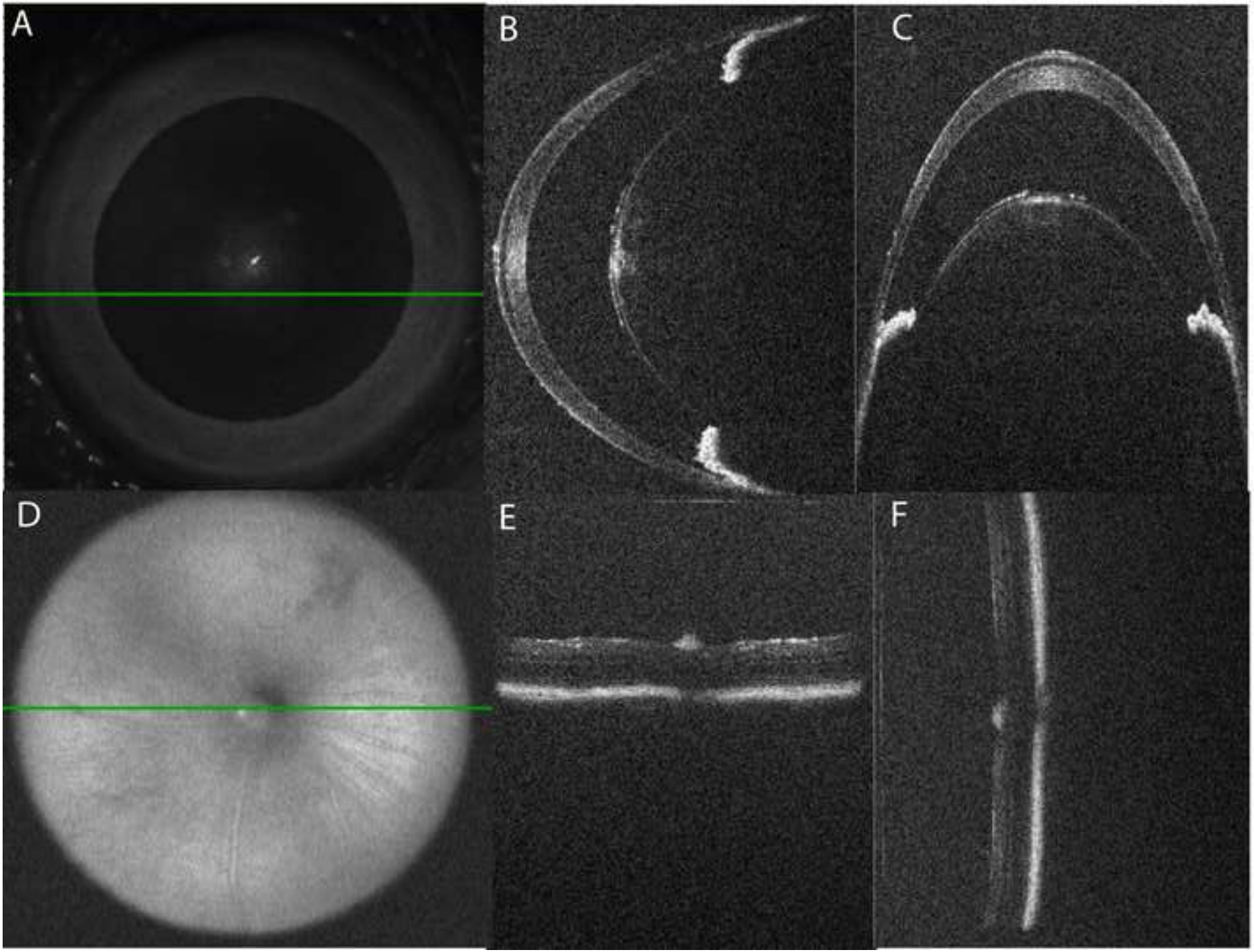

Figure 3

Click here to access/download;Figure;Figure 3.jpg

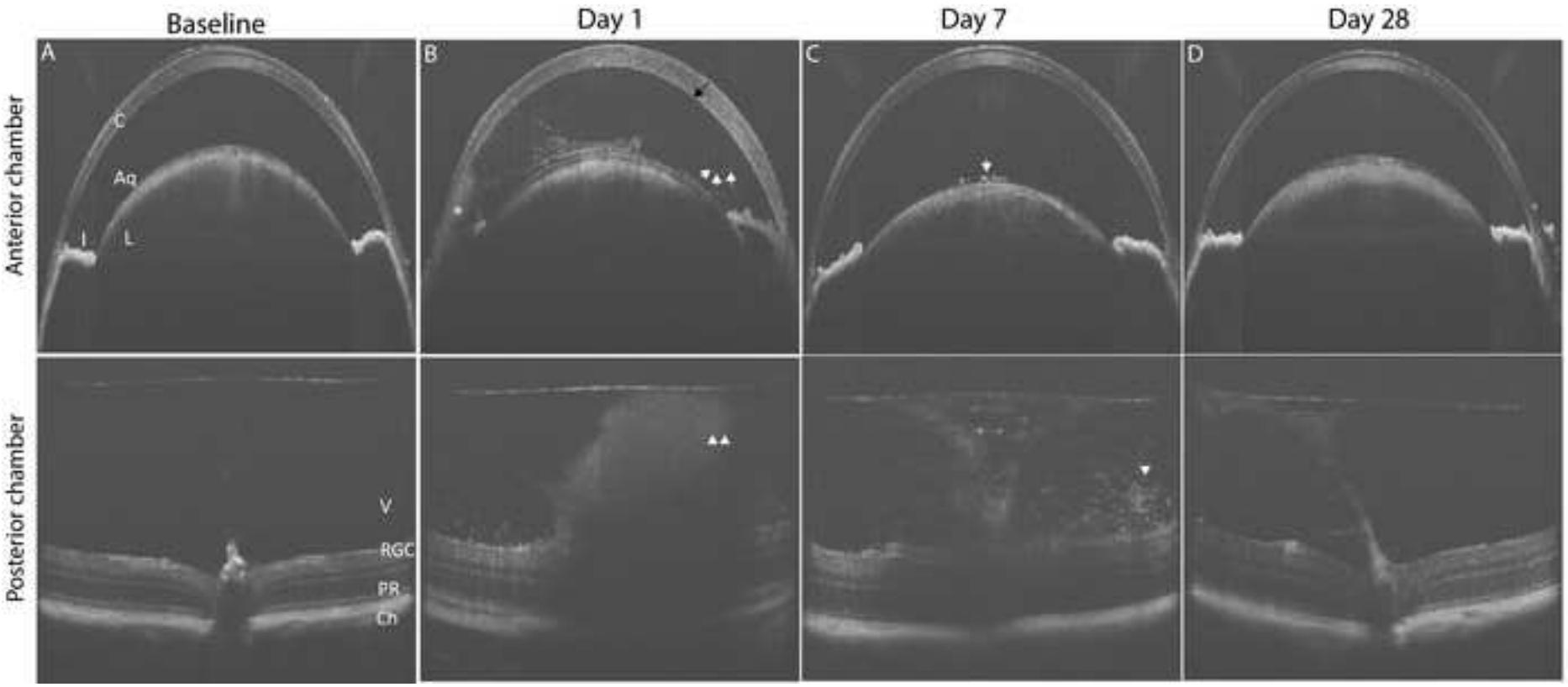

Figure 4

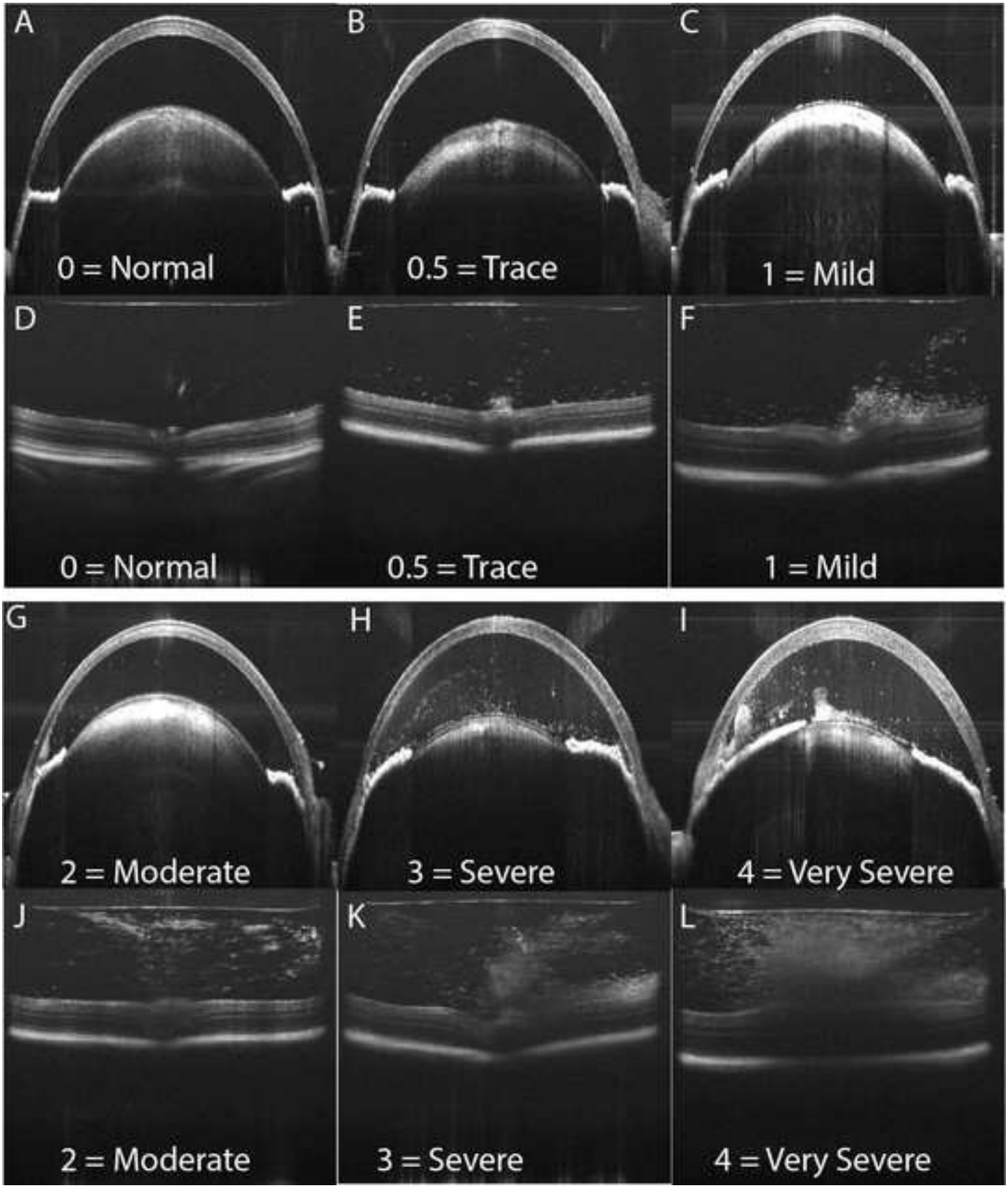

Figure 5

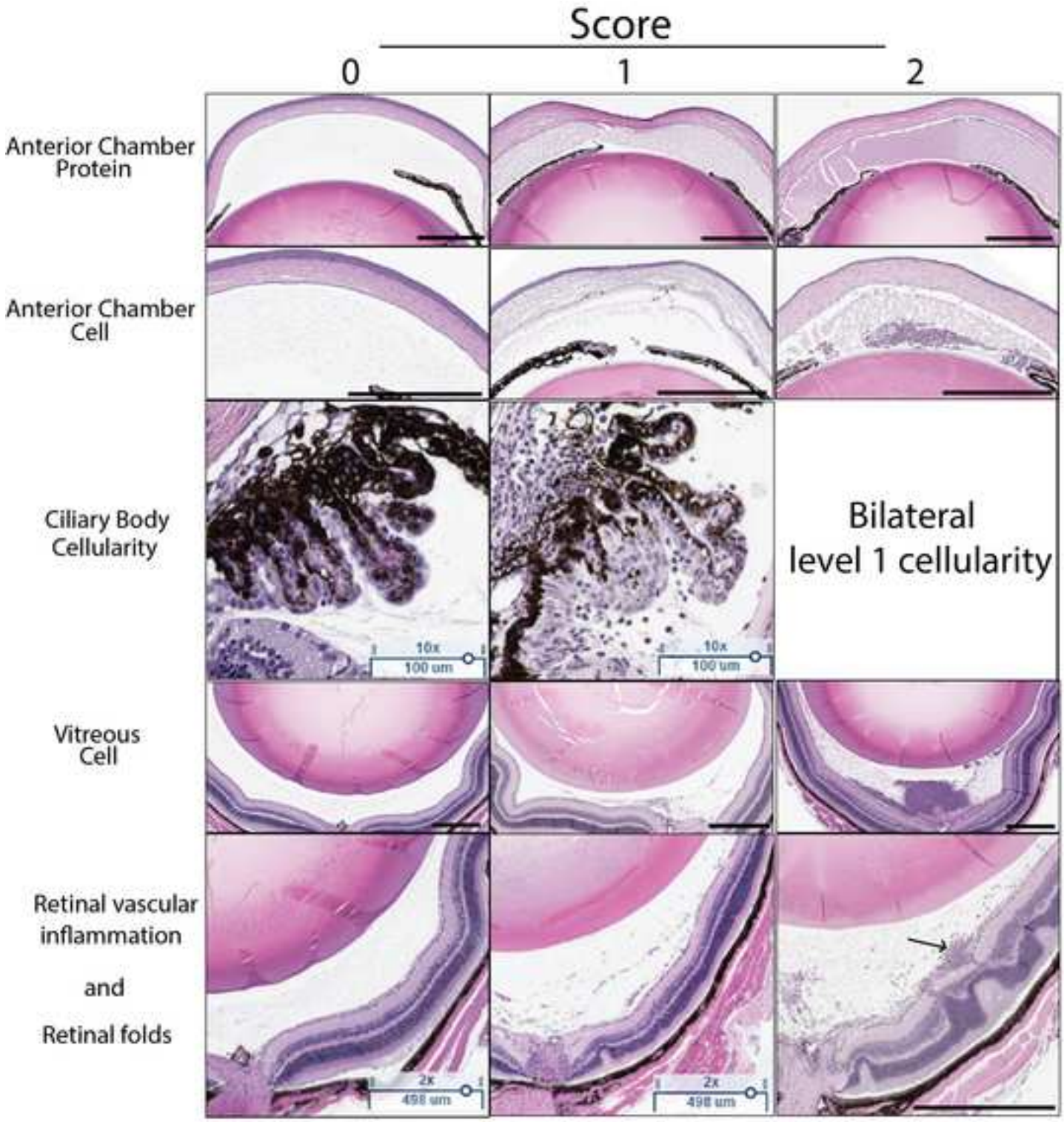

Figure 6

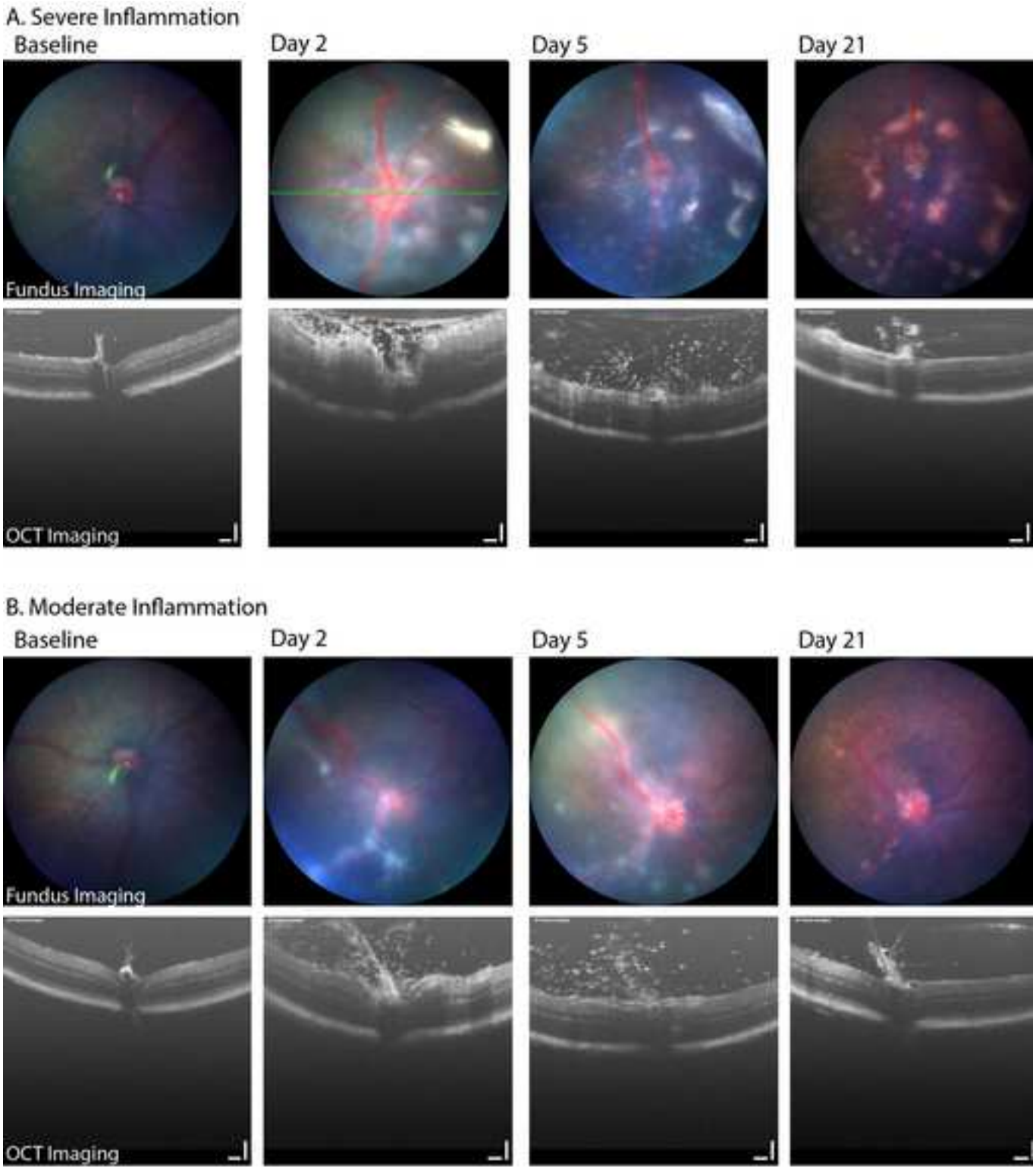

Table 1

A

Mouse Anterior Chamber	**Fast Scan**	**Volume Scan**	**Linear Scan**
Length X Width	4.0 mm x 4.0 mm	3.6 mm x 3.6 mm	3.6 mm
Angle	0	90	90
A-scan/B-Scan	800	1000	1000
# B-scans	50	400	1
Frames/ B-scan	1	3	20
Mouse Posterior Chamber	**Fast Scan**	**Volume Scan**	**Linear Scan**
Length X Width	1.6 mm x 1.6 mm	1.6 mm x 1.6 mm	1.6 mm
Angle	0	0	0
A-scan/B-Scan	800	1000	1000
# B-scans	50	200	1
Frames/ B-scan	1	3	20

B

Mouse Posterior Chamber	**Volume Scan**	**Linear Scan**
Length X Width	0.9 mm x 0.9 mm	1.8 mm
Angle	0	Any (typically 0 or 90)
A-scan/B-Scan	1024	1024
# B-scans	512	1
Frames/ B-scan	1	30

	OCT Score descriptions	
Score	**Anterior Chamber**	**Posterior Chamber**
NA	No view beyond anterior cornea	No view of posterior segment
0	No inflammation	No inflammation
0.5	1–5 cells in the aqueous OR corneal edema	Few cells occupying less than 10% of the vitreous area No subretinal or intraretinal infiltrates or retinal architecture disruption
1	6–20 cells in the aqueous OR a single layer of cells on the anterior lens capsule	Diffuse cells (no dense clumps) occupying between 10 and 50% of the vitreous area. No subretinal or intraretinal infiltrates or retinal architecture disruption
2	20–100 cells in the aqueous OR fewer than 20 cells and a hypopyon present	Diffuse cells (no dense clumps) occupying > 50% of the vitreous area No subretinal or intraretinal infiltrates or retinal architecture disruption
3	20–100 cells in the aqueous AND a hypopyon OR a pupillary membrane	Diffuse cells equal to grade 2 and 1 AND at least one dense vitreous opacity occupying 10%–20% of the vitreous area OR the presence of vitreous cells equal to grade 2 and rare (≤ 2) subretinal or ntraretinal opacities
	Any number of aqueous cells	Dense vitreous opacity occupying > 20% of the vitreous area.

4	AND a large hypopyon and pupillary membrane OR anterior structure loss due to severe inflammation	OR diffuse vitreous cells with large subretinal or intraretinal opacities

Table 3

	Histology Score Description		
Characteristic	**0**	**1**	**2**
Anterior Chamber (AC) Protein	Scant acellular particles staining with eosin in the AC	Moderate, but not confluent, extracellular eosin staining anywhere in the AC	Confluent or near confluent extracellular eosin staining throughout the AC
Anterior Chamber (AC) Cell	No cells	1–100 cells, but no dense aggregations of cells	>100 cells, or dense aggregations of cells
Ciliary Body Inflammation	No leukocyte infiltration of the ciliary body or surrounding vitreous	Unilateral presence of leukocytes infiltrating the ciliary body and/or the surrounding vitreous.	Bilateral presence of leukocytes infiltrating the ciliary body and/or the surrounding vitreous.
Retinal Vascular Inflammation	No retinal vessels with perivascular leukocytes	One vessel per section with perivascular leukocytes	>1 vessel per section with perivascular leukocytes
Retinal fold or damage	No retinal damage	1–3 retinal folds per section	>3 retinal folds per section, or any other retinal layer destruction or intraretinal hemorrhage

Reviewer's comment	Response	Text changes
1. Please take this opportunity to thoroughly proofread the manuscript to ensure that there are no spelling or grammar issues.	DONE	
2. Please revise the text to avoid the use of any personal pronouns (e.g., "we", "you", "our" etc.).	DONE	
3. JoVE cannot publish manuscripts containing commercial language. This includes trademark symbols (™), registered symbols (®), and company names before an instrument or reagent. Please remove all commercial language from your manuscript and use generic terms instead. All commercial products should be sufficiently referenced in the Table of Materials.For example: Eppendorf, NanoFil, Ultra Micro Pump, SilFlex, AK-Fluor, Bioptigen/Leica, Micron, etc.	Eppendorf changed to microcentrifuge tubes, NanoFil deleted, Ultra Micro Pump changed to micropump, SilFlex deleted, AK-Fluor, Bioptigen/Leica, Micron are deleted in the protocol but mentioned in Table of Materials. Genteal replaced by 0.3% hypromellose gel.	Product details are added on Table of Materials.
4. Please adjust the numbering of the Protocol to follow the JoVE Instructions for Authors. For example, 1 should be followed by 1.1 and then 1.1.1 and 1.1.2 if necessary. Please refrain from using bullets or dashes.	DONE	
5. Please ensure that all text in the protocol section is written in the imperative tense as if telling someone how to do the technique (e.g., “Do this,” “Ensure that,” etc.). The actions should be described in the imperative tense in complete sentences wherever possible. Avoid usage of phrases such as “could be,” “should be,” and “would be” throughout the Protocol. Any text that cannot be written in the imperative tense may be added as a “Note.” However, notes should be concise and used sparingly. Please include all safety procedures and use of hoods, etc.	DONE	
6. For time units, please use abbreviated forms for durations of less than one day when the unit is preceded by a numeral throughout the protocol. Do not abbreviate day, week, month, and year. Examples: 5 h, 10 min, 100 s, 8 days, 10 weeks	DONE	

7. Line 97: Please specify what kind of Biosafety cabinet. Class, type,etc. Please ensure that steps of caution are mentioned in the protocol.	DONE	1.1 : "Perform all procedures in this section inside a chemical fume hood under sterile conditions to prevent inhalation of the Mtb H37Ra powder. This includes using chemical resistant gloves, safety glasses and protective work clothing (lab coat)".
8. Line 105-109: Is there any specific type of probe to be used. Include specifications like size, length, etc. Any specific conditions like frequency, amplitude etc.?	Text added to Methods section.	1.4: "First, unclamp the body of the converter unit and clean the probe with a 70% (v/v) alcohol swab. Then switch on the sonicator, adjust the power setting to 4 by turning the power control knob and immerse the tip of the probe into the PBS-containing mycobacterial powder. Ensure that the probe tip is immersed to at least half the depth of the sample and that the probe tip is not touching the wall of the microcentrifuge tube. Sonicate the mixture on ice for 30 secs, pause 30 secs and repeat for a total of 5 min to fully disperse into suspension without heating the liquid. After sonication, set the power to 0 using the control knob and wipe the probe with alcohol swab after turning off the unit".

9. Line 123: What does day 7 represent. 7 days of acclimatization?	We apologize for any confusion. We have rewritten this line to improve clarity. There are seven days between the subcutaneous injection and the intravitreal injection. The day of subcutaneous injection had been indicated as day -7. Due to this confusion it is now written as "one week prior to intravitreal injection".	2.1: "Subcutaneous injection is performed a week prior to the intravitreal injection (designated as day -7)".
10. Being a video-based journal, JoVE authors must be very specific when it comes to the humane treatment of animals. Regarding animal treatment in the protocol, please add the following information to the text:		
a) Please include an ethics statement before all of the numbered protocol steps indicating that the protocol follows the animal care guidelines of your institution.	DONE	Ethics statement is included in the beginning of the protocol.
b) Please specify the euthanasia method.	Text added to protocol	"Animal euthanasia was performed using the carbon dioxide inhalation method 30".
c) Please mention how animals are anesthetized and how proper anesthetization is confirmed.	Text added to protocol	2.4 To perform the subcutaneous injection safely, either anesthetize the mouse or utilize humane restraint methods that allow easy access to the animal hindquarters. 31 To anesthetize for subcutaneous injection, the animal is placed in an isoflurane induction chamber (3-4% for induction and 1-3% for maintenance). Once anesthetized, the mouse should have a slow respiratory rate and should

		not exhibit any signs of respiratory distress.
d) Please specify the use of vet ointment on eyes to prevent dryness while under anesthesia.	Text added to protocol	Indicated in step 4.1.7, “cover the eye with hypromellose (0.3%) or carbomer eye gel (0.2% w/w) to prevent dryness under anesthesia. This will also help to prevent cataract formation."
e) For survival strategies, discuss post-surgical treatment of animal, including recovery conditions and treatment for post-surgical pain.	Text added to protocol	Section 4.3.11-4.3.13. Remove the mouse from the platform, place 0.3% hypromellose or 0.2% w/w carbomer on both eyes for corneal protection, and move to the recovery warming box. Do not leave the mouse unattended until it has regained sufficient consciousness to maintain sternal recumbency. When the mouse is fully awake, return to the cage and add acetaminophen (200–300 mg/kg/day) medicated water bottle. Label cage card with date of IVT injection.
f) Discuss maintenance of sterile conditions during survival surgery.	Text added to protocol	3.1 "Perform all procedures in this section under appropriate sterile conditions to prevent contamination" and 4.1.6 "Perform all procedures in this section under appropriate sterile

		conditions to prevent endophthalmitis."
g) Please specify that the animal is not left unattended until it has regained sufficient consciousness to maintain sternal recumbency.	Text added to protocol	Added to 2.6, 4.3.12 and 5.2.13
h) Please specify that the animal that has undergone surgery is not returned to the company of other animals until fully recovered.	Text added to protocol	4.3.12 Do not leave the mouse unattended until it has regained sufficient consciousness to maintain sternal recumbency. Do not return to the company of other animals until fully recovered.
i) Please do not highlight any steps describing euthanasia.	DONE	
11. Line 222: Please mention if this step is to be performed in the dark?	Thank you for this question. The fluorescein is not light sensitive and does not need to be performed in the dark.	no text edits
12. Please include a one-line space between each protocol step and then highlight up to 3 pages of the Protocol (including headings and spacing) that identifies the essential steps of the protocol for the video, i.e., the steps that should be visualized to tell the most cohesive story of the Protocol. Remember that non-highlighted Protocol steps will remain in the manuscript, and therefore will still be available to the reader.	DONE, we might want to discuss additional steps in the video planning stages.	
13. Figures: Please use Uppercase alphabets to label the images of the panel.	DONE	
14. Figure 1: Please remove the commercial terms from the figure and the figure legends and replace them with generic terms.	DONE	
15. Figure 2: Does the green line represent the volume intensity projection. Please specify in the figure legends. Please remove the commercial terms from the figure legends.	Sorry for the confusion. To clarify, the green line marks the location of the line scan that is being shown in the panel immediately to the right of the en-face	"Figure 2: Proper alignment of the eye for OCT imaging. (A) Using the en-face scanning laser ophthalmoscope (SLO) image the eye is centered for anterior chamber imaging. The green line

	image. For example the green line in figure 2A indicates where the image in 2B was obtained and the green line in image 2D is the same as 2E. This information has been added to the figure legend.	indicates the position of the horizontal line scan shown in panel (B)".
16. Figure 5: Please include scale bars in all the images of the panel. Define the magnification in the figure legends.	DONE. We have placed a black scale bar on all images that did not have the scale indicated. This scale bar is 500 microns in length. This information has been added to the figure legend.	
17. Figure 6: Please mention which of these images are fundal and OCT. Annotations are not seen in the images but mentioned in the figure legends. Please ensure that details of magnification, scale bars, etc. are included in the figure legends.	DONE	
18. Table 1: Please maintain a single spacing between the number and unit (e.g., “4.0 mm x 4.0 mm”)	DONE	
19. Please revise the table of the essential supplies, reagents, and equipment. The table should include the name, company, and catalog number of all relevant materials in separate columns in an xls/xlsx file. Please sort the Materials Table alphabetically by the name of the material. Please remove trademark (™) and registered (®) symbols from the Table of Equipment and Materials.	DONE	
_____		
Reviewers' comments:		

Reviewer #1:		
Major Concerns:		
The most important concern is about the research application of this model. Can it substitute the more expensive rabbit and rat models of PMU that were used for studies on intravitreal injections? Presumably, it cannot.	Thank you for this observation. It is true that one of the big benefits of using the smaller mouse model is the difference in cost. For some applications, the mice can replace the larger more expensive models. All the rodent models can be used for pre-clinical therapy testing if the agent is administered systemically or as a topical drop. However, since the mouse model has a much smaller eye than the rat or rabbit model some local therapy options are not able to be tested. For example, surgically placed ocular implant studies are usually only performed in the rabbit model. Both the rabbit and rat models can be used for testing local therapy options such as intravitreal therapy which would be more challenging in the mouse model.	Text added to the discussion to address this point: "One of the advantages of using the mouse model is the ready availability of numerous transgenic and knockout strains that can help understand the basic mechanism of uveitis (Agarwal et al. 2012). All rodent models can be used for pre-clinical therapy testing if the agent is administered systemically or as a topical drop. However, due to their larger size, rat and rabbit eyes are better models for use in pre-clinical studies of implantable or local injection treatment options for uveitis".
The authors have projected it as a model of chronic post-infectious uveitis, in this case tuberculosis. In my opinion, it is important to specify the infection (and not use a generic post-infectious), since TB is the primary antigen for inducing intraocular inflammation. However	We have specifically addressed each point below.	

there are several differences that separate it from human ocular TB infections:		
1. Human ocular TB pathogenesis is a complex process that is not fully understood. However, there is a clear role of live mycobacteria in the eye or elsewhere, judging from the therapeutic benefit of anti-TB therapy in these patients. Hence, killed mycobacterial extract as the starting material does not seem promising. It is surprising that the authors have not cited papers on animal models of ocular TB from recent and historical literature (PMiD: 32407249, 33010848).	We agree the pathogenesis of human TB associated uveitis is complex and incompletely understood. We acknowledge that PMU does not model all the aspects due to active infection, we think it is reasonable to use the heat killed mTB as a proxy for the residual non-viable Mtb or its components that would remain after appropriate ATT. These non-viable components have been suggested to trigger immune responses underlying the aspects of disease that respond to corticosteroid treatment.(PMID 33010848, Basu et al. Sep. 2020) The articles referenced by the reviewer have been included in the introduction.	Text added to Introduction: "Presence of granulomatous inflammation in the posterior segment of the eye suggests that the PMU model can be used to study some forms of anterior (granulomatous and non-granulomatous) and intermediate uveitis, seen in patients with immunological evidence of past Mtb infection. (Basu et al. 2020). Additionally, the components of heat killed Mtb used in the PMU model have been suggested to trigger immune responses underlying the aspects of recurrent uveitis in patients with ocular tuberculosis who respond to anti-tubercular therapy (ATT)(Basu et al. 2020)" .

2. The inflammation in PMU is mainly anterior uveitis and vitritis - both of which are generally not seen in isolation in ocular TB (though in the mouse model, the authors have reported retinal vasculitis)	Ocular TB in humans has been reported to cause all forms of uveitis. We agree that mouse models are often incomplete in recapitulating all aspects of disease in humans. PMU can capture some manifestations seen in humans like granulomatous inflammation and presence of lymphocyte infiltrate. However, it should be used in conjunction with other models for the complete picture.	Text added to Introduction: "Presence of granulomatous inflammation in the posterior segment of the eye suggests that the PMU model can be used to study some forms of anterior (granulomatous and non-granulomatous) and intermediate uveitis, seen in patients with immunological evidence of past Mtb infection. (Basu et al. 2020).
3. The primary immune response in the acute stage is innate and consists of myeloid cells/neutrophils - again not a feature of ocular TB, where we see primarily a lymphocytic infiltrate	We have clarified in the discussion section that in the PMU model, acute neutrophil dominant inflammation subsides by day 7. After the first week, T cells are the dominant CD45+ cell in the eye which is consistent with findings in humans.	Text added: "In the PMU model, acute inflammation is characterized by an innate response with a predominant neutrophil infiltrate, followed by a chronic and persistent adaptive T cell dominant response that persists for over a month.46 (John et al. 2020)
4. The intraocular cytokine response is also very different from ocular TB - both IL-17 and TNFa are high in ocular TB, which is not the case in PMU	The reviewer is addressing our prior finding in rats that did not identify elevated IL-17. We have new data (currently unpublished) that does identify elevated levels of IL-17, TNF-a, and other key inflammatory cytokines in the eyes of mice. The manuscript with this	no additional edits

	data will be published shortly (elsewhere) and we think will help support the relevance of the model to future investigators. Reporting these results here are beyond the scope of this methods oriented manuscript.	
Multiple injections were used in the rat and rabbit models to maintain chronic inflammation - this has not been mentioned for the mouse model. Will this model be used for studying mainly the acute or chronic inflammation	Repeat injections are not advisable in the mouse due to its small size. In the PMU model, the mouse eye does provide chronic disease out to 56 days without repeat injections. Therefore it can be used as a mixed model to study both innate and adaptive arms of immune response in the eye.	Text added: "In the PMU model, acute inflammation is characterized by an innate response with a predominant neutrophil infiltrate, followed by a chronic and persistent adaptive T cell dominant response that persists for over a month.46 (John et al. 2020)
The point on retinal vasculitis is not clear. This was not seen in the rabbit/rat models - how do the authors explain it for the mouse model? This seems closer to EAU than PMU	Excellent question and an important observation. We have not studied the rabbit model ourselves, so we cannot be sure that retinal vasculitis does not occur, although it has not been reported. In our prior studies we used Lewis rats which have an albino fundus which can make detection or	no additional edits

	retinal or retinal vascular disease more difficult to appreciate on fundus exam. It is possible there is retinal vascular inflammation in the rat model that has not been completely described. In humans vitreous inflammation (intermediate uveitis) is often accompanied by retinal vascular inflammation, so this finding in the mouse is consistent with aspects of human disease.	
Minor Concerns:		
How do the authors ensure reproducibility of aqueous cell counts on OCT	The cells themselves are not counted individually in the mouse eye. Instead, three masked graders evaluate each image and assign a score based on the criteria in table # and shown in figure #. We presented this reproducibility data at the ARVO conference this year (Abstract # 3542743), but in brief we found high inter-grader agreement and excellent intra-grader reproducibility suggesting the score system is robust.	

Reviewer #2:		
Minor Concerns:		
1. Regarding the subcutaneous injection of Mtb; do control mice receive a similar sham injection? Also, if mice are anaesthetised for this injection, it might be worthwhile to apply Genteal or gel drops to prevent corneal drying.	Depending on the experimental question, there are a number of PBS "sham" injection controls that could be considered. We have performed PBS "sham" intravitreal injections in animals that received subcutaneous Mtb and compared the results to animals injected with intravitreal Mtb. We have not explored the impact of sham subcutaneous PBS injection prior to intravitreal Mtb injection. We have added a list of sham controls to consider during experimental design to the discussion section. We do routinely provide corneal protection during all anesthesia event, and have updated the methods to reflect this concern.	Text edits to discussion: "Controls should be selected to ensure results are due to the response to mTB and not trauma associated with the subcutaneous or intravitreal injections. In the sham injection controls, PBS can be used in place of the mTB extract. For comparisons to unexposed animals, true naive samples should be considered as fellow eyes are not always equivalent". Text edit to 4.7 "Remove betadine and cover the eye with hypromellose (0.3%) or carbomer eye gel 0.2% w/w) to prevent dryness under anesthesia. This will also help to prevent cataract formation that can result if the cornea becomes dry".
2. What is the rationale for anaesthetising the cornea for OCT imaging, which is a non-contact procedure?	We have noted that the iris dilation and anterior chamber visualization is improved when topical anesthesia is administered. We suspect that the corneal reflex to touch is better suppressed with the	Text edits to 4.4- "Note: It has been observed that iris dilation and anterior chamber visualization is improved when topical anesthesia is administered, possibly due to improved corneal reflex suppression with the combined systemic and topical anesthesia. However, this

	combined systemic and topical anesthesia, however this step could be omitted if desired. We have updated methods to explain this rational.	step could be omitted if desired".
3. In Figure 4C, the lens appears cataractous. Is this a consequence of the anaesthesia, or a feature of mild inflammation?	This is a very good question. We have not studied the incidence of cataract in the model. It is possible it is associated it with inflammation, but it is probably due to anesthesia artifact. We occasionally see this degree of cataract even in baseline images which we have attributed to anesthesia.	no text edits

4. The information provided in Table 2 is very useful for scoring inflammation by OCT imaging. It would be good to indicate how many frames should be analysed per eye- particularly as there can be variability in the distribution of inflammatory cells in the anterior chamber (with perhaps a bias towards the inferior AC due to gravity). This would be particularly relevant for the milder grades of inflammation.	Thank you for this insightful question. We agree there can be region differences in the degree of inflammation, and this has been reported previously by others. We have dealt with this by orienting our imaging to capture both the inferior and superior aspects of the anterior chamber in the same images. (ie our line scans are oriented vertically) This orientation information is provided in Table 1, note the parameter for "angle" in Table 1a indicates the 90 degree orientation for capturing the volume and line scan. We have highlighted this aspect in the legend of figure 4. We have also added a recommendation to considering using at least 3 line scans for scoring to ensure regional variability is captured. Alternatively, reviewing the volume scan to confirm that the central line scan is representative can be a reasonable option to limit the number of images that require masked scoring.	Text added to discussion: "Prior reports have identified an uneven distribution of cells in the anterior chamber of humans with more cells located inferiorly (Li et al. 2013). In mice, a similar predisposition is common. Thus, vertical or radial scans through the AC will help ensure images that capture the range of inflammation. Additionally, performing imaging in the same place will also provide consistency to images collected in the same eye longitudinally. To obtain images in the same part of the eye, use stable landmarks and a systematic approach. For anterior chamber images, the image is centered immediately adjacent to the apex of the cornea and oriented vertically so that the presence of a hypopyon can be detected in the inferior angle. For posterior segment images, the image is centered on the optic nerve. It is recommended to consider using at least 3 line scans for scoring to ensure regional variability is captured. In cases where inflammation is restricted to peripheral locations, acquiring volume scans can be helpful. Collection of volume scans can also be helpful in capturing regional variations, but will increase data storage requirements".

Editor’s comment:	Our response:
1. Please note that the manuscript has been formatted to fit the journal standard. The numbering of the protocol steps is adjusted, and repeated steps in different sections of the protocol are referenced as step numbers to avoid repetition of steps. Comments to be addressed are included in the manuscript itself. Please review and revise accordingly.	Revisions addressed.
2. Figure 5: The histology image corresponding to ciliary body cellularity under the score 2 panel (bilateral level 1 cellularity) is missing. Please include an image. Please confirm whether all the scale bars are 500 µm. The images of ciliary body cellularity show a scale bar of 100 µm. Please confirm whether it is correct and include a description in the figure legend stating that the scale bars for the ciliary body cellularity images indicate 100 µm.	The figure legend has been edited to clarify the scale bars. To clarify, there is not an image in the score 2 location intentionally. We have clarified in the figure legend and the text of the results section. The reader is instructed to use the level 1 score to determine cellular infiltration of the ciliary body. If this feature is noted in the ciliary body sections present on both sides of the lens in a single section, this is termed "bilateral involvement" of the ciliary body in that section. This then gives the eye the score level of 2.
3. Please ensure that the Table of Materials contains all the essential supplies, equipment, and reagents used in the study (e.g., sectioning instrument).	This is done.
4. As two authors have affiliations in the UK please sign the UK Author License Agreement attached with this email and upload it along with the revised submission.	This version has been signed.

jove JOURNAL OF VISUALIZED EXPERIMENTS
1 Alewife Center #200
Cambridge, MA 02140
tel. 617.945.9051
www.jove.com

ARTICLE LICENSE AGREEMENT

Title of Article: Primed Mycobacterial Uveitis (PMU) as a Model for Post-Infectious Uveitis

Author(s): Sarah John, Oliver H. Bell, Leslie Wilson, David A. Copland, Kathryn L. Pepple

Item 1: The Author elects to have the Article be made available (as described at https://www.jove.com/authors/publication) via:

☐ Standard Access ☒ Open Access

Item 2: Please select one of the following items:

☒ The Author is **NOT** a United States government employee.

☐ The Author is a United States government employee and the Article was prepared in the course of his or her duties as a United States government employee.

ARTICLE LICENSE AGREEMENT

1. **Defined Terms.** As used in this Article License Agreement, the following terms shall have the following meanings: "**Agreement**" means this Article License Agreement; "**Article**" means the manuscript submitted by Author(s) and specified on the last page of this Agreement, including texts, figures, tables and abstracts; "**Author**" means the author who is a signatory to this Agreement; "**Collective Work**" means a work, such as a periodical issue, anthology or encyclopedia, in which the Article, along with a number of other contributions, constituting separate and independent works in themselves, are assembled into a collective whole;"**CRC License**" means the Creative Commons Attribution 4.0 Agreement (also known as CC-BY), the terms and conditions of which can be found at: https://creativecommons.org/licenses/by/4.0/; "**CRC NonCommercial License**" means the Creative Commons Attribution-NonCommercial 3.0 Agreement (also known as CC-BY-NC), the terms and conditions of which can be found at: http://creativecommons.org/licenses/by-nc/3.0/legalcode; "**Derivative Work**" means a work based upon the Article and other pre-existing works, such as a translation, musical arrangement, dramatization, fictionalization, motion picture version, sound recording, art reproduction, abridgment, condensation, or any other form in which the Article may be recast, transformed, or adapted; "**Institution**" means the institution, listed on the last page of this Agreement, by which the Author was employed at the time of the creation of the Article; "**JoVE**" means MyJove Corporation, a Delaware corporation and the publisher of Journal of Visualized Experiments; "**Parties**" means the Author and JoVE.

2. **Background.** The Author, who is the author of the Article, in order to ensure the review, Internet formatting, publication, dissemination and protection of the Article, desires to have JoVE publish the Article. In furtherance of such goals, the Parties desire to memorialize in this Agreement the respective rights of each Party in and to the Article.

3. **Grant of Rights in Article.** In consideration of JoVE agreeing to review, arrange and coordinate the peer review, format, publish and disseminate the Article, the Author hereby grants to JoVE, subject to **Sections 4** and **8** below, the exclusive, royalty-free, perpetual license (a) to publish, reproduce, distribute, display and store the Article in all forms, formats and media whether now known or hereafter developed (including without limitation in print, digital and electronic form) throughout the world, (b) to translate the Article into other languages, create adaptations, summaries or extracts of the Article or other Derivative Works or Collective Works based on all or any portion of the Article and exercise all of the rights set forth in (a) above in such translations, adaptations, summaries, extracts, Derivative Works or Collective Works and(c) to license others to do any or all of the above. The foregoing rights may be exercised in all media and formats, whether now known or hereafter devised, and include the right to make such modifications as are technically necessary to exercise the rights in other media and formats.

4. **Retention of Rights in Article.** The Author shall, with respect to the Article, retain the non-exclusive right to use all or part of the Article for the non-commercial purpose of giving lectures, presentations or teaching classes, and to post a copy of the Article on the Institution's website or the Author's personal website, in

each case provided that a link to the Article on the JoVE website is provided and notice of JoVE's copyright in the Article is included. All non-copyright intellectual property rights in and to the Article, such as patent rights, shall remain with the Author.

5. **Grant of Rights in Article – Standard Access.** This **Section 5** applies if the "Standard Access" box has been checked in **Item 1** above or if no box has been checked in **Item 1** above. In consideration of JoVE agreeing to review, arrange and coordinate the peer review, format, publish, and disseminate the Article, the Author hereby acknowledges and agrees that, Subject to **Section 8** below, JoVE is and shall be the sole and exclusive owner of all rights of any nature, including, without limitation, all copyrights, in and to the Article. To the extent that, by law, the Author is deemed, now or at any time in the future, to have any rights of any nature in or to the Article, the Author hereby disclaims all such rights and transfers all such rights to JoVE.

If the Author's funding is a subject to the requirement of the NIH Public Access Policy, JoVE acknowledges that the Author retains the right to provide a copy of their final peer-reviewed manuscript to the NIH for archiving in PubMed Central 12 months after publication by JoVE. If the Author's funding is subject to the requirement of the RCUK Policy, JoVE acknowledges that the Author retains the right to self-deposit a copy of their final Accepted Manuscript in any repository, without restriction on non-commercial reuse, with a 6-month embargo, and under the CRC NonCommercial License.

Notwithstanding anything else in this agreement, if the Author's funding is a subject to the requirements of Plan S, JoVE acknowledges that the Author retains the right to provide a copy of the Author's accepted manuscript for archiving in a Plan S approved repository under a Plan S approved license.

6. **Grant of Rights in Article – Open Access.** This Section 6 applies only if the "Open Access" box has been checked in Item 1 above. If the Author's funding is subject to the requirement of the RCUK Policy, JoVE and the Author hereby grant to the public all such rights in the Article as provided in, but subject to all limitations and requirements set forth in the CRC License.

7. **Government Employees.** If the Author is a United States government employee and the Article was prepared in the course of his or her duties as a United States government employee, as indicated in **Item 2** above, and any of the licenses or grants granted by the Author hereunder exceed the scope of the 17 U.S.C. 403, then the rights granted hereunder shall be limited to the maximum rights permitted under such statute. In such case, all provisions contained herein that are not in conflict with such statute shall remain in full force and effect, and all provisions contained herein that do so conflict shall be deemed to be amended so as to provide to JoVE the maximum rights permissible within such statute.

8. **Protection of the Work.** The Author(s) authorize JoVE to take steps in the Author(s) name and on their behalf if JoVE believes some third party could be infringing or might infringe the copyright of the Article.

9. **Privacy, Personality.** The Author hereby grants JoVE the right to use the Author's name, picture, photograph, image, biography, likeness, voice and performance in any way, commercial or otherwise, in connection with the Articles and the sale, promotion and distribution thereof.

10. **Author Warranties.** The Author represents and warrants that the Article is original, that it has not been published, that the copyright interest is owned by the Author (or, if more than one author is listed at the beginning of this Agreement, by such authors collectively) and has not been assigned, licensed, or otherwise transferred to any other party. The Author represents and warrants that the author(s) listed at the top of this Agreement are the only authors of the Article. If more than one author is listed at the top of this Agreement and if any such author has not entered into a separate Article License Agreement with JoVE relating to the Article, the Author represents and warrants that the Author has been authorized by each of the other such authors to execute this Agreement on his or her behalf and to bind him or her with respect to the terms of this Agreement as if each of them had been a party hereto as an Author. The Author warrants that the use, reproduction, distribution, public or private performance or display, and/or modification of all or any portion of the Article does not and will not violate, infringe and/or misappropriate the patent, trademark, intellectual property or other rights of any third party. The Author represents and warrants that it has and will continue to comply with all government, institutional and other regulations, including, without limitation all institutional, laboratory, hospital, ethical, human and animal treatment, privacy, and all other rules, regulations, laws, procedures or guidelines, applicable to the Article, and that all research involving human and animal subjects has been approved by the Author's relevant institutional review board.

11. **JoVE Discretion.** If more than one author is listed at the beginning of this Agreement, JoVE may, in its sole discretion, elect not take any action with respect to the Article until such time as it has received complete, executed Article License Agreements from each such author. JoVE reserves the right, in its absolute and sole discretion and without giving any reason therefore, to accept or decline any work submitted to JoVE. JoVE has sole discretion as to the method of reviewing, formatting and publishing the Article, including, without limitation, to all decisions regarding timing of publication, if any.

12. **Indemnification.** The Author agrees to indemnify JoVE and/or its successors and assigns from and against any and all claims, costs, and expenses, including attorney's fees, arising out of any breach of any warranty or other representations contained herein. The Author further agrees to indemnify and hold harmless JoVE from and against any and all claims, costs, and expenses, including attorney's fees, resulting from the breach by the

jove JOURNAL OF VISUALIZED EXPERIMENTS
1 Alewife Center #200
Cambridge, MA 02140
tel. 617.945.9051
www.jove.com

ARTICLE LICENSE AGREEMENT

Author of any representation or warranty contained herein or from allegations or instances of violation of intellectual property rights, damage to the Author's or the Author's institution's facilities, fraud, libel, defamation, research, equipment, experiments, property damage, personal injury, violations of institutional, laboratory, hospital, ethical, human and animal treatment, privacy or other rules, regulations, laws, procedures or guidelines, liabilities and other losses or damages related in any way to the submission of work to JoVE, or publication in JoVE or elsewhere by JoVE. All indemnifications provided herein shall include JoVE's attorney's fees and costs related to said losses or damages. Such indemnification and holding harmless shall include such losses or damages incurred by, or in connection with, acts or omissions of JoVE, its employees, agents or independent contractors.

13. **Fees.** To cover the cost incurred for its work, JoVE must receive payment before publication of the Article. Payment is due 21 days after invoice. Should the Articles not be published due to the JoVE's decision, these funds will be returned to the Author. If payment is not received before the publication of the Article, the publication will be suspended until payment is received.

14. **Transfer, Governing Law.** This Agreement may be assigned by JoVE and shall inure to the benefits of any of JoVE's successors and assignees. This Agreement shall be governed and construed by the internal laws of the Commonwealth of Massachusetts without giving effect to any conflict of law provision thereunder. This Agreement may be executed in counterparts, each of which shall be deemed an original, but all of which together shall be deemed to me one and the same agreement. A signed copy of this Agreement delivered by facsimile, e-mail or other means of electronic transmission shall be deemed to have the same legal effect as delivery of an original signed copy of this Agreement.

A signed copy of this document must be sent with all new submissions. Only one Agreement is required per submission.

CORRESPONDING AUTHOR

Name:	Kathryn Pepple
Department:	Ophthalmology
Institution:	University of Washington
Title:	Associate Professor
Signature:	[signature]
Date:	8/31/2021

Please submit a **signed** and **dated** copy of this license by one of the following three methods:

1. Upload an electronic version on the JoVE submission site
2. Fax the document to +1.866.381.2236
3. Mail the document to JoVE / Attn: JoVE Editorial / 1 Alewife Center #200 / Cambridge, MA 02140